AN ELECTROCHEMICAL STUDY OF THE KINETIC AND THERMODYNAMIC PROPERTIES OF 6-(DIFERROCENYLHEXANYLCARBONYL)PENTANETHIOL SELF-ASSEMBLED MONOLAYERS

by

Wendy L. Lewis

Submitted in Partial Fulfillment of the Requirements

for the Degree of

Master of Science

in the

Chemistry

Program

Youngstown State University

August, 2002

AN ELECTROCHEMICAL STUDY OF THE KINETIC AND THERMODYNAMIC PROPERTIES OF 6-(DIFERROCENYLHEXANYLCARBONYL)PENTANETHIOL SELF-ASSEMBLED MONOLAYERS

by

Wendy Lewis

I hereby release this thesis to the public. I understand that this thesis will be made available from the OhioLINK ETD Center and the Maag Library Circulation Desk for public access. I also authorize the University or other individuals to make copies of this thesis as needed for scholarly research.

Signature

Wendy L. Lewis 8/9/02

Wendy L. Lewis, Student Date

Approvals

Larry S. Curtin 8/2/02

Larry S. Curtin, Ph.D., Thesis Advisor Date

Timothy R. Wagner 7/26/02

Timothy R. Wagner, Ph.D., Committee Member Date

James H. Mike 8/2/02

James H. Mike, Ph.D., Committee Member Date

Peter J. Kasvinsky 8/7/02

Peter J. Kasvinsky, Ph.D., Dean of Graduate Studies Date

ABSTRACT

Monolayers of 6-(diferrocenylhexanylcarbonyl)pentanethiol (DFHC6SH) were formed on gold electrodes and the kinetic and thermodynamic parameters associated with electron transfer were investigated via cyclic voltammetry (CV). The voltammograms in 1.0 M $HClO_4$ (aq) displayed two peaks centered at approximately 90 mV and 390 mV vs. Ag/AgCl, associated with oxidation of the outer and inner ferrocene groups, respectively. The measured formal potentials were characteristic of carbonyl and akyl substituted ferrocenes. Both of the oxidations were found to be chemically and electrochemically reversible on the voltammetric time scale. In addition, FWHM values for both electron transfers were determined to be significantly larger than the theoretical value of 90/n mV, indicating that the monolayers were somewhat disordered. This conclusion was also supported by the inability to measure a heterogeneous electron transfer rate constant for the outer ferrocene.

The surface coverage for the inner ferrocene group was determined to be approximately 7 x 10^{-11} mole/cm^2, a value which is typical for a monolayer containing an electroactive terminal group which occupies a volume as large as diferrocenylhexane. The surface coverage for the outer ferrocene moiety was found to be approximately 40-50% of that for the inner ferrocene, indicating that many of the outer ferrocene sites are electrochemically inaccessible. This is of great interest because it is the opposite of what was observed by Mirken et. al., where an outer ferrocene group was fully accessible and an inner azobenzene group was totally inaccessible.[27]

This unusual phenomenon was explored by comparing the voltammetry in 1.0 M $HClO_4$ (aq) with that obtained in 0.10 M TBAP/THF electrolyte. Use of the less polar, aprotic solvent caused the surface coverages for both ferrocenes to decrease by approximately 40-60% due to desorption. The *ratio* of the surface coverages for the inner and outer ferrocenes, however, was found to be the same as that obtained in aqueous electrolytes, indicating that the electrochemical inaccessibility of the outer ferrocenes was probably not due to them folding into the non-polar hexane bridge.

Ion-pairing thermodynamics were also probed by obtaining cyclic voltammograms in 1.0 M H_2SO_4 (aq) solutions containing varying amounts of perchloric acid.[10] The formal potentials for both ferrocene groups were observed to shift anodically with decreasing perchloric acid concentrations. Plots of the formal potentials vs. $\log_{10}$ [$HClO_4$] were used to obtain the ion-pairing constants for the two ferrocenes. The values of K_{eff} for the inner and outer ferrocenes were determined to be 13.06 M^{-1} and 3.915 M^{-1}, respectively. The values were much smaller than those reported by Creager et. al., indicating that DFHC6SH monolayers are more disordered than the mixed monolayers employed by Creager.[10] In addition, the larger K_{eff} measured for the inner ferrocenes reflects the increased "alkane-like" environment caused by the bridging hexane group.

ACKNOWLEDGEMENTS

I would like to start off by thanking my parents. Without their love and support this project would not have been possible. They always encouraged me to stick with school, even when I felt like quitting. I would also like to thank my brothers, Matt and Adam, for their support and for giving me a break from school when I needed it. I also owe a great deal of gratitude to my grandma and grandpa Miller, who always believed in me. I would also like to thank them for letting me live with them my last semester. What would Sunday nights be without a card game? I would like to thank my grandma and grandpa Lewis in Las Vegas for their love and support. Even if they don't live near by, they always took the time to let me know they care. I would like to thank the rest of my family, both in Ohio and outside, for their support. I would like to thank my friends Adam and Bonnie for listening to me and for their support and encouragement.

I would like to thank Dr. Curtin for all of his help the past couple of years. Without his help, this project would never have gotten off the ground. I would also like to thank the rest of the Curtin research group, Carolyn Pugh, Jeff Meyers, Valerie Copanic, and Rick Porter for their help. They are a great group to work with and are always willing to lend a hand. I would like to thank Dr. Wagner for the use of his tube furnace and vacuum pump. Special thanks goes out to Ray Hoff for helping with the various instruments and being the "fix-it" guy when they are broken. I would like to thank my committee for taking the time to

read my thesis and make corrections. And finally, I would like to thank Youngstown State University for funding my research.

Table of Contents

List of Figures

Chapter 1: Introduction

1.1 Introduction to Self-Assembled Monolayers

A modified electrode can be made from either electroactive or electroinactive species, with the ability to tailor the electrode/solution interface at the molecular level. Self-assembled monolayers (SAMs) spontaneously form ordered systems that are one molecule thick.[1, 2] General properties include a head group that can form a covalent bond with, or have non-bonding interactions with, a substrate. Another property is that the terminal group can be electroactive or electroinactive. The length of the alkane chain separating the head and terminal groups can also be varied. The chemical and physical properties of the monolayer are dramatically affected by each of the components that comprise the monolayer. There are a variety of methods used to make self-assembled monolayers, each with their own advantages and disadvantages.

Because so many different types of compounds with different properties can be attached to electrodes, this is an interesting area of chemistry to study. Fundamental studies can be done in interfacial science, electron transport, and charge transport.[3, 4, 5, 6] Also, the monolayers themselves have a variety of likely exploitations; including chemical and biological sensors, corrosion prevention, soft lithography, and molecular electronic and non-linear optical device technologies.[7]

An electroactive head group that is connected to an electrode by an ordered, insulating alkane chain is often used in fundamental studies in interfacial science

and in potential applications.[8] If the head group is covalently bound to the surface of the SAM, then the monolayers have proven to be more robust for potential applications (see Figure 1.1).[7]

1.2 Langmuir-Blodgett (L-B) Films

One way to build up organic monolayers and multilayers is the Langmuir-Blodgett (L-B) technique. Although this method is technically not self-assembly, it can be used to build molecular layers on a surface. Langmuir-Blodgett monolayers, which are not covalently bound to a substrate, are formed when amphiphilic molecules are spread on an air/liquid or liquid/liquid interface and are subsequently compressed onto a solid substrate (see Figure 1. 2).[7] Making an L-B film is a delicate process that can be done by immersing a hydrophilic glass substrate into an aqueous solution containing amphiphilic molecules. After immersion, the slide is gently drawn out of solution and the layer is compressed in an L-B trough. This results in an ordered film with a hydrophilic substrate and a hydrophobic end which is perpendicular to the surface.

In L-B films, the head group is not covalently bonded to the surface. The monolayer is formed as a result of weak electrostatic interactions with the substrate. These weak interactions increase the number of degrees of freedom of the molecules, allowing the monolayer to be compressed on the surface. The absence of a covalent bond leads to films that have numerous defects and are not very stable or reproducible. These films have a tendency to collapse easily

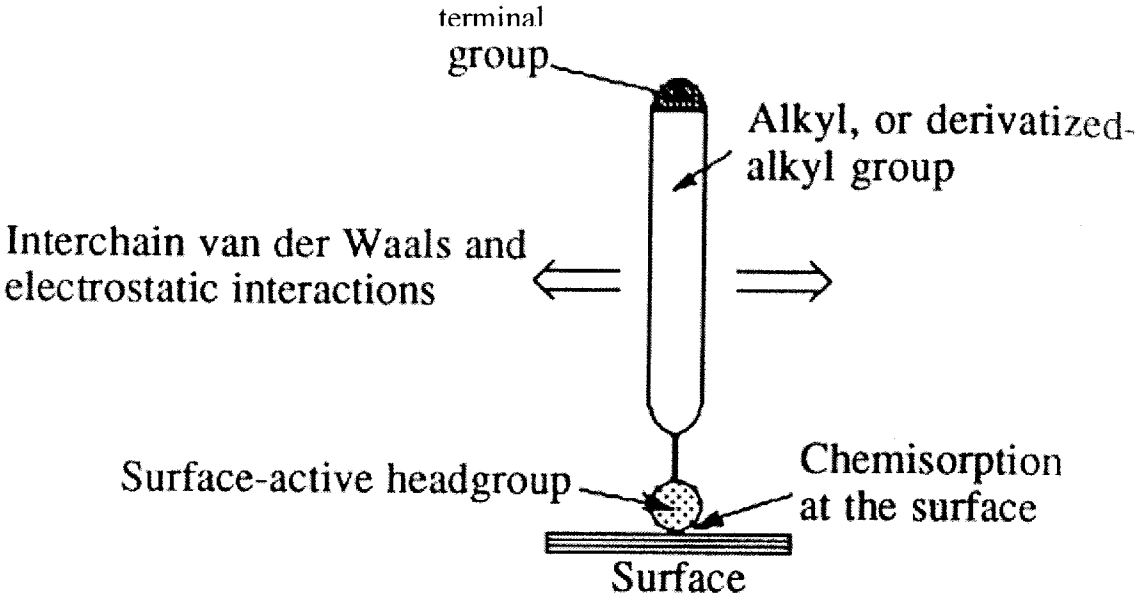

Figure 1.1: Schematic representation of the groups that comprise a typical monolayer. Reprinted from reference 4.

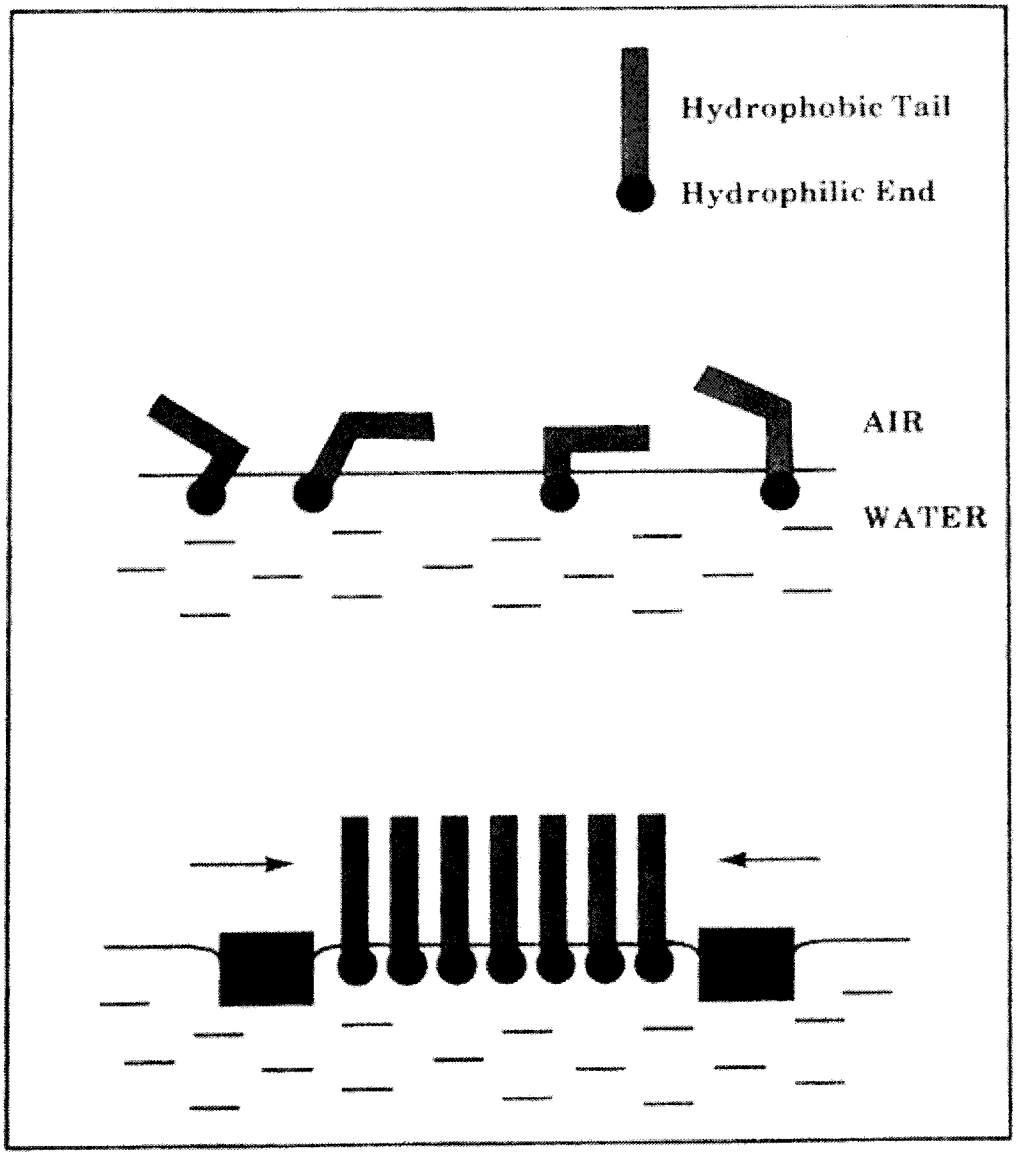

Figure 1.2: Schematic of Langmuir-Blodgett techniques. Reprinted from reference 4.

and can be readily removed from the substrate, leading to limited use for practical applications.

Things such as the environment, the subphase, the amphiphiles, and cleaning between experiments can have a profound affect on L-B film formation, especially because they are not covalently bound to the surface.[9] A sophisticated L-B trough and a laminar hood are typically used to form L-B films, which are other disadvantages to this technique.[9]

The alkane chain length can affect the order of the film. An increase in the chain length increases the order of the film and also increases stability to an extent. This is because as the chain length is increased, the number of defect sites decreases because of increased van der Walls interactions between the alkane chains. The increased interaction causes the molecules to pack more densely on the surface, thus decreasing the number of defect sites, and increasing the order of the monolayer.

The terminal group can also affect the physical and chemical properties of the monolayer. For example, a methyl group can be used to produce a hydrophobic surface or a hydroxyl group can be used to make a hydrophilic surface. Specific properties can be generated from a monolayer when certain electroactive or photoactive terminal groups attached.[3, 10] In particular, the size and physical and chemical properties of the chain terminus have been shown to have a dramatic affect on the ordering and stability of the films, and also on their potential applications.

Langmuir-Blodgett methods can also be used to make multilayer films. This is done by repetitive exposure to amphiphilic solutions and subsequent compression of the films. In this case, the non-polar end of the original monolayer interacts with the non-polar end of the next layer. The bi-layer is then exposed to another amphiphilic solution, resulting in a tri-layer. Repetition of this process can lead to films with a variety of sizes and applications.

There are advantages to making L-B films. Monolayers can be made in which the monolayer/air or monolayer/surface interface can be adjusted to give desired properties. Also, the mobility of the monolayer can be good for studying electron transfer.

There are also some significant disadvantages to making L-B monolayers. The film is not covalently bound to the surface, which makes them unstable, hard to reproduce, and sensitive to environmental conditions. These disadvantages, along with the need for expensive, specialized equipment, make L-B films impractical for useful applications.

1.3 Organosilanes

Silanes can also be used to make chemically modified surfaces. This technique comprises bonding between trichloro- or triethoxysilane derivatives and a surface that is hydroxylated.[9] Surfaces such as Pt, silica, or high temperature superconductors are typical examples of substrates that can be used. Spontaneous chemisorption occurs on the surface, resulting in more robust films

than those produced by L-B techniques. These silanes form true self-assembled monolayers. The chemical and physical properties, order, stability, and applications of these monolayers can be affected by the head group, alkyl chain, and the terminal group (see Figure 1.3).

Covalent bonding increases the overall stability of the monolayer as compared to L-B films. There are problems with this bond, however. The bonding with the surface is not well defined and there can be polymeric cross-linking to the surface. This causes the size of the head group to be much bigger than that of the alkane chain, which leads to disorder and problems with reproducibility. In addition, the head group is very reactive which can cause problems due to sensitivity to water.

The length of the alkyl chain will affect the order of the monolayer. Despite the fact that longer akyl chains tend to be more ordered, the indeterminate nature of the bonding to the electrode still causes some disorder in all silane monolayers. Murray et. al. performed experiments with long chain ferrocene-terminated organosilanes and proved that disorder is present even in monolayers containing long alkyl chains.[11] The study demonstrated that the electron transfer kinetics associated with oxidation of the ferrocene terminal group was electrochemically reversible on the voltammetric time scale, indicating that the monolayer was significantly disordered. This disorder is due to the size of the head group and terminal group being much larger than the alkyl chain. Generally, the terminal group doesn't have as much of an affect on the order of

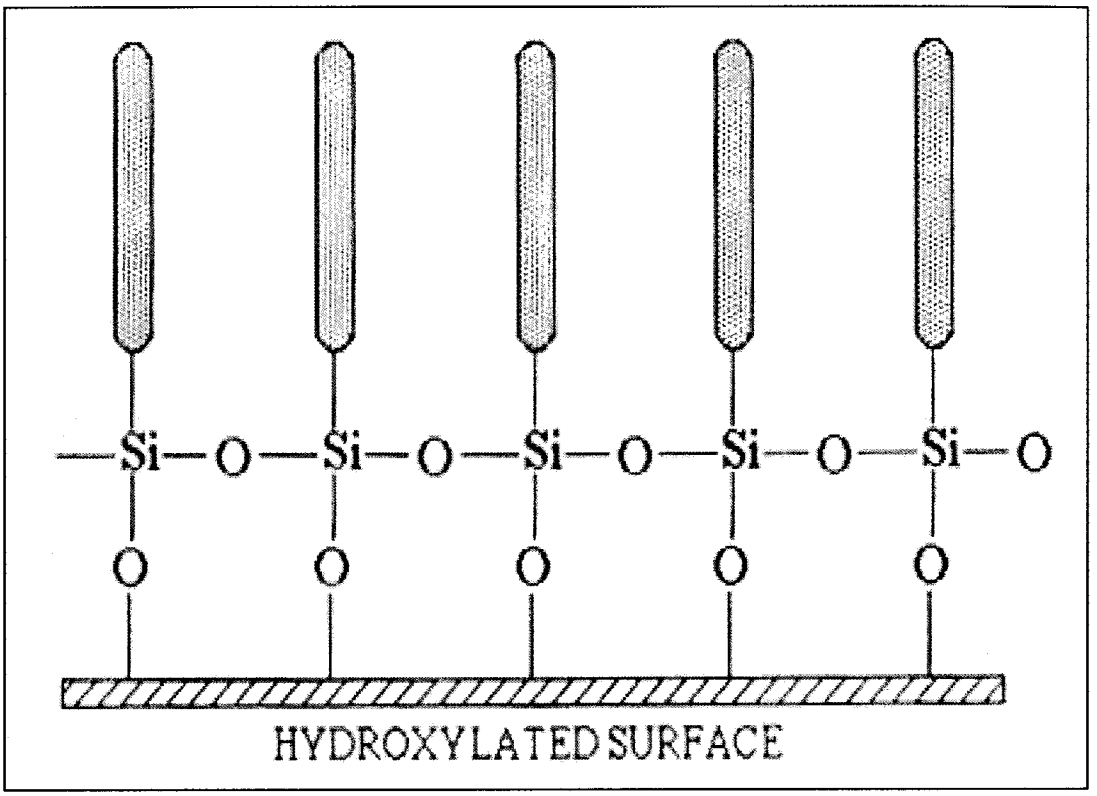

Figure 1.3: Schematic for the formation of an organosilane. Reprinted from refererence 4.

the monolayer as the head group, because it is better defined than the headgroup.

There are a variety of uses for silanes. R_2SiX_2 and R_3SiX organosilanes, in which X is either a halogen or an alkoxy group, have been covalently bonded to hydroxylated surfaces, which have been used as bonded phases for liquid and gas chromatography.[9] They have also been used for enzyme immobilization. $(CH_3)_3SiCl$ and $(CH_3)_2SiCl_2$ can also be used in making the hydrophobic surfaces used in L-B films.[9]

Organosilane SAM's have many advantages over L-B films. The strong covalent bond makes the monolayer much more robust than L-B films. They are also easier to prepare than L-B films because no specialized equipment is needed, all that is necessary is to soak the surface in a coating solution containing the organosilane.

There are also some disadvantages to using silanes. $Si(OC_2H_5)_3$ and $SiCl_3$ groups are very reactive towards water, leading to difficulties in preparing quality silane films in open air. Thus, a glove bag or box is typically required. Another disadvantage is disorder in the monolayer as a result of the size of the head group and the polymeric nature of the surface. Also the $SiCl_3$ and $Si(OC_2H_5)_3$ groups are fairly reactive, making them difficult to couple to a variety of terminal groups.

1.4 Alkanethiol SAMs

Alkanethiol SAMs contain a thiol head group, an alkane chain of variable length, and a variety of terminal groups that can be attached (see Figure 1.4). Alkanethiol SAMs are more practical than L-B films or silanes because they are fairly easy to make and there is no need for specialized equipment. SAMs form spontaneously when the electrode, which is typically gold or silver, is soaked in a dilute alkanethiol solution overnight. By making specific changes on the molecular level, it is possible to produce monolayers that have desired chemical and physical properties.

The gold-sulfur covalent bond that forms is strong (c.a. 30-35 kcal/mole).[12] This is the primary driving force for monolayer formation. The strong bond that forms when the thiol chemisorbs to the substrate causes the monolayer to be much more robust than L-B films, making them more attractive for practical applications.

The size of the sulfur atom is about the same as the diameter of the alkane chain, which allows the films to be more ordered, if the correct conditions are used. This makes them more practical than silanes for most applications. Also, alkanethiol monolayers are air and water stable. Another advantage is that they are synthetically easy to couple to a variety of terminal groups. This allows for the production of monolayers with many different properties, without the need for specialized equipment.

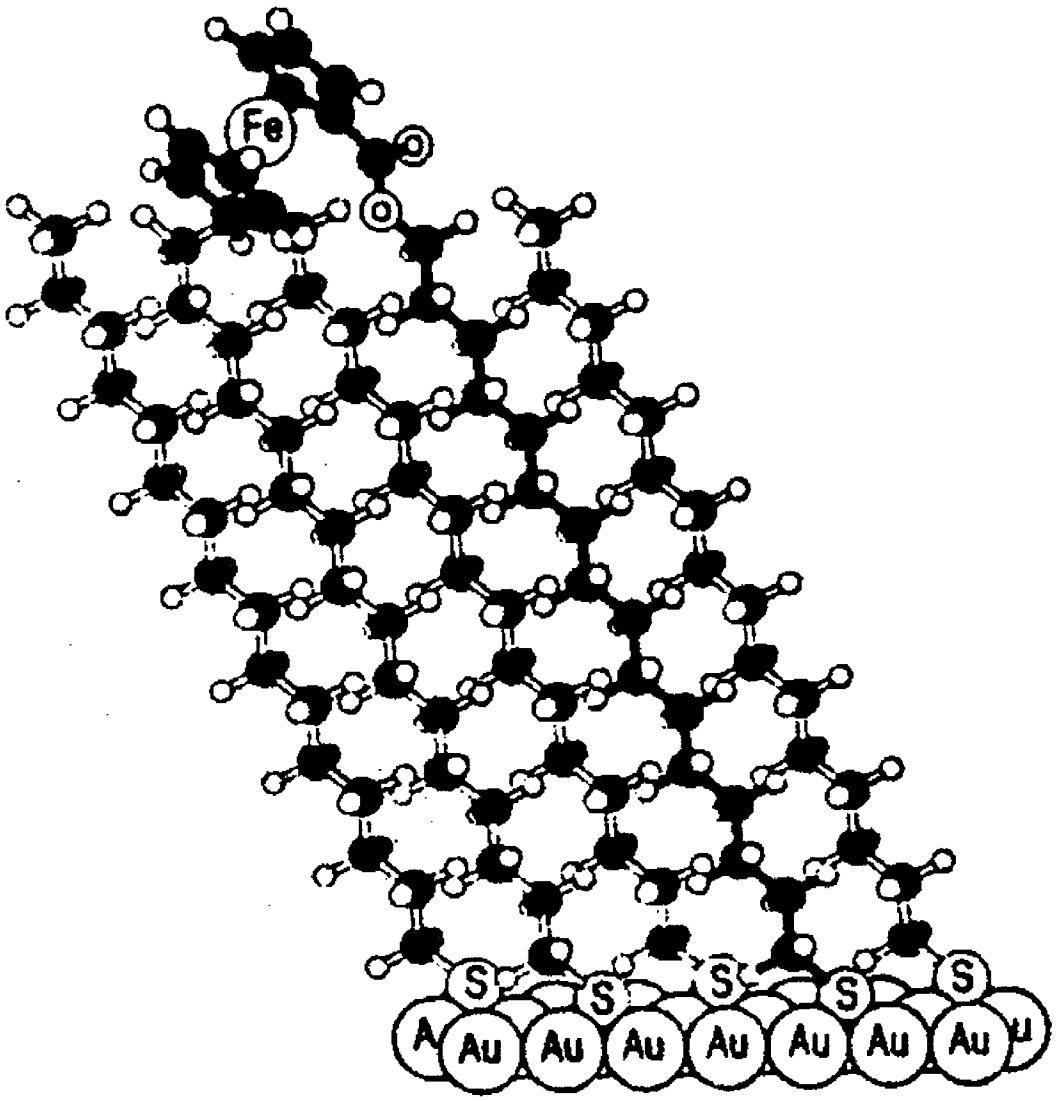

Figure 1.4: A schematic of a typical alkanethiol monolayer. Reprinted from reference 4.

A variety of surfaces can be used to make self-assembled alkanethiol monolayers. Au, Ag, Cu, Pt, and Hg are common examples. A strong covalent bond is formed between the thiol and the surface, which gives stable monolayers. The monolayers can pack differently depending on the nature of the surface, and this will have a dramatic effect on the ordering of the monolayer. Even monolayers formed on the same type of metal can have large differences in ordering, depending on the exposed crystal face. For example, alkanethiol SAMs on Au(111) substrates pack in a hexagonal $\sqrt{3}$ X $\sqrt{3}$ R30° array in which the thiol adsorbates are spaced 5.0 Å apart.[3] Alakanethiol SAMs on Au(100) pack in a base-centered square array c(10 X 10) where the S-S bond distance is 4.54 Å.[13] In both cases it is possible to obtain crystalline monolayers under the appropriate circumstances. It is difficult to obtain crystalline monolayers on a polycrystalline surface because the broad distribution of crystal faces leads to disorder.

Van der Waals interaction between alkane chains is the secondary driving force for monolayer ordering. Ordering of the SAM can be determined by electrochemistry, contact angle goniometry, surface IR, ellipsometry, X-Ray diffraction, and neutron diffraction.[9, 14, 15] An increase in the van der Waals forces between adjacent alkanes occurs with increasing chain length, which leads to an increase in the order of the monolayer. Alkane chains of 1-6 methylene units tend to be disordered, chains of 6-12 methylene units are somewhat ordered, and chains of more than 12 carbons in length can be truly crystalline. Chidsey

used helium diffraction to demonstrate that on Au (111) surfaces, the alkane chains extend in all *trans* configurations with tilt angle of 27° with respect to the surface normal.[3,16] This angle allows the alkyl chains to pack more densely, resulting in a monolayer which is truly crystalline.

Contact angle measurements are made by placing a drop of liquid on the surface and measuring the angle that the liquid makes with the surface. The liquid and the surface can be either polar or non-polar, which will affect the contact angle. If the surface is hydrophilic, then a water drop will spread out on the surface, resulting in a small contact angle. If the surface is hydrophobic, then the surface will repel the water and it will bead up, much like water on a freshly waxed car, thus increasing the contact angle. Longer alkane chains will be more hydrophobic, thus repelling the water and having larger contact angles.[17] Therefore, if the contact angle is large it implies the presence of a more ordered monolayer.

Ellipsometry is often used to measure the thickness of monolayer films by using polarized light.[9] Light separates into its parallel and perpendicular parts when it comes in contact with a surface. Depending on the surface, the amplitude and phase of the light will vary. The perpendicular and parallel portions of the light together give elliptically polarized light. From this information, the thickness of a thin film between the surface and air can be found. The angles and the thickness are relative to the refractive index, which is typically estimated. A refractive index of 1.50 is recommended for simple alkyl

chains of C_{10} or longer, whereas if a metal is added, refractive indices higher than 1.50 are recommended. For akyl chains of C_9 or shorter, refractive indices of less than 1.50 are recmmended.[9] Rabe and Knoll were able to measure differences in thickness to 2 Å.[18]

FTIR can also be used to investigate the effect of chain length on a monolayer by probing the local environment in the SAM.[9] Cyrstalline alkanes display symmetric and asymmetric CH_2 stretching modes at 2851 cm^{-1} and 2918 cm^{-1}, respectively.[19] Long chain alkanethiol monolayers display the same stretching frequencies, implying a high degree of order. As the chain length is decreased, the stretching frequencies shift to higher wavenumbers, indicating an increase in disorder. The results of FTIR studies of alkanethiol SAMs confirm that short alkane chains ($n \leq 9$) are liquid like, and it would follow that such a system would be more prone to thermally induced disorder.[9] Results of surface IR studies are often confirmed by other methods such as X-ray and neutron diffraction.

Another advantage displayed by alkanethiol SAMs with respect to silane monolayers is that thiols are synthetically easy to couple to a wide variety of electroactive terminal groups such as ferrocenes, viologens, anthroquinones, and ruthenium pentammines. Thus, they allow electrochemical techniques to be used as indirect probes for structure/property correlations in self-assembled monolayers.

The chemical and physical properties of monolayers depend on chain length, the nature of the head group, the terminal group, the substrate, and the surface

structure. In general, compared to techniques such as Langmuir-Blodgett films and other SAMs, alkanethiol SAMs are more practical because they do not have problems with stability and reproducibility as seen in Langmuir-Blodgett films, or problems with ordering as seen with silanes.

1.5 Electrochemistry

Electrochemical techniques are popular investigative tools because they can easily measure the kinetic and thermodynamic properties of compounds. Also, electrochemical techniques can measure low concentrations of analytes. Electrochemistry is commonly used to examine SAMs or other modified surfaces with just a single layer attached because it provides structure/property correlations.

Electrochemistry is the science of charge and electron transfer. One can examine both chemical and electrochemical processes. Charge transfer reactions can be either heterogeneous and homogeneous.[14, 20] In these reactions, an oxidation is always accompanied by a reduction. An oxidation occurs with the loss of electrons and a reduction occurs with the gain of electrons.

A minimum of two electrodes are necessary for electrochemistry. The electrode of interest is the working electrode and the other electrode (for the other half-reaction) is the counter electrode. In addition, a reference electrode is commonly used to accurately control the potential of the working electrode.[14, 21]

Consider the reduction of O to R:

$$O + ne^- \rightarrow R$$

This reaction takes place at the working electrode. The other half reaction, which is often not well understood, occurs at the counter (or auxiliary) electrode. Current flows between the working and counter electrodes because the electrons given up in the oxidation reaction at the counter electrode are used in the reduction reaction at the working electrode. A potentiostat is used to control the difference in potential between the working and counter electrodes. A negligible amount of current flows between the working and the reference electrodes because a large impedance is arranged between the reference and working electrodes. If current were to flow between the working and reference electrodes, then the concentration of the species inside the reference electrode would change, leading to a change in the potential of the reference electrode. The potential difference between the working and reference electrode is measured throughout the scan by the potentiostat and is adjusted as needed.

Some examples of working electrodes are Au, Pt, and glassy C. These substrates are used because they are inert over relatively wide potential ranges, which means that they do not play an active role in the electrochemistry; they are simply supplying or removing electrons. The choice of working electrode can affect the kinetics of an electron transfer reaction and therefore affect the overpotential which must be applied to drive the reaction. As a result, the choice of the electrode affects the potential window in which reactions can take place. Typical counter electrodes are also inert metals, such as Au or Pt. Some often-

used reference electrodes are aqueous based saturated calomel and Ag/AgCl electrodes, or non-aqueous based Ag/Ag^+ electrodes.

Cyclic voltammetry is a powerful electrochemical technique for a variety of reasons. The simplicity and ease of data analysis makes it possible to readily extract thermodynamic and kinetic parameters associated with electron transfer. In cyclic voltammetry, a linear potential ramp is applied to the working electrode at a given scan rate until a pre-determined switching potential is achieved. In the reverse scan the potential is generally brought back to the initial potential at the same scan rate (see Figure1.5). The resulting voltammogram is a plot of current response versus the applied potential. A typical CV for the reduction of a monolayer-coated electrode is shown in Figure 1.6.

Initially the potential is not negative enough to initiate the reduction of O to R. As the potential of the working electrode is made more negative, the ions in solution migrate in response to the change in the electrode potential. This motion of charge results in non-Fardaic currents, which are associated with ion migration and not electron transfer. The magnitude of the non-Faradaic currents limit the sensitivity of the experiment by reducing the signal to noise ratio. If the non-Faradaic currents are large, then the analyte's signal can be overwhelmed by the background current. In addition, non-Faradaic currents limit the time scale of the experiments because the electrical double layer at the working electrode must be fully charged before the potential of the working electrode can be known accurately.

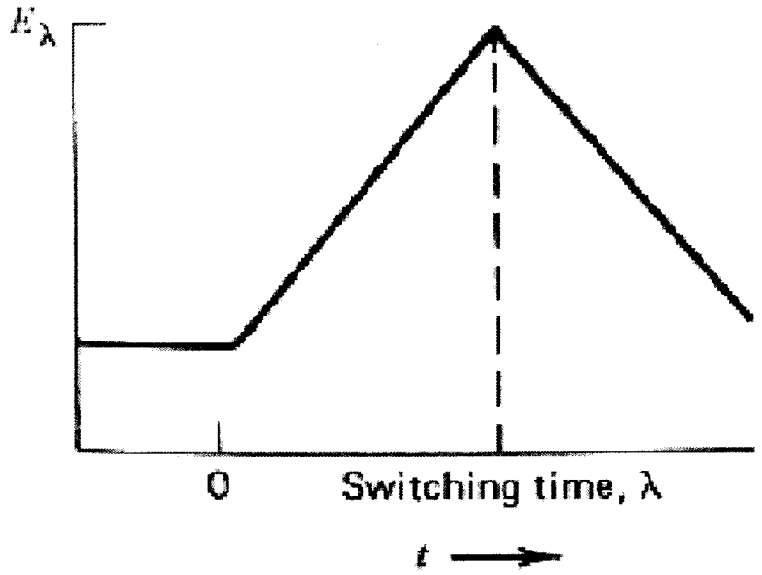

Figure 1.5: Plot of potential v. time. Reprinted from reference 4.

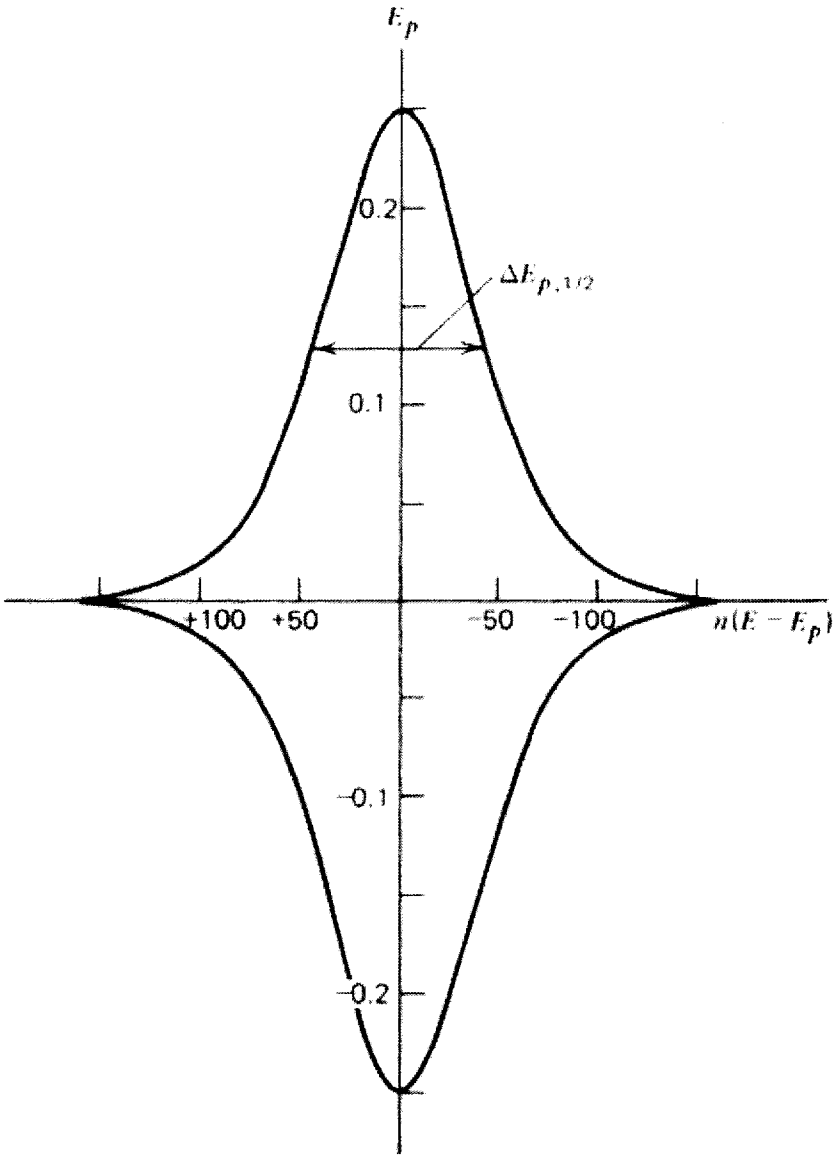

Figure 1. 6: Typical cyclic voltammogram. Reprinted from reference 4.

As the potential of the working electrode is made increasingly negative, the energy of the electrons that are in the metal escalates until it becomes thermodynamically favorable for the electrons to transfer from the metal to the analyte. This results in the reduction of O to R (see Figure 1.7).[14] The currents that are involved in electron transfer to and from the analyte are Faradaic currents, which are typically the currents of interest. When analyzing self-assembled monolayers, the current increases until half the species are reduced, where it reaches a maximum value. After reaching this value, the current decreases until all of the species have been reduced.

When this point is reached, non-Faradaic currents only occur until the switching potential is reached. The potential scan is then reversed, making the electrode more positive. Eventually, the potential of the working electrode becomes sufficiently positive to re-oxidize the species which were reduced in the forward scan. As before, the Faradaic current increases to a maximum value and then decreases to background levels, at which point the original monolayer has been regenerated.

Faradaic currents are used to study chemical and electrochemical kinetics. An electrochemically reversible electron transfer is defined as one that is rapid, based on the time scale of the experiment. An electrochemically reversible reduction reaction will follow the Nernst equation at all applied potentials.

$$E = E^\circ + RT/nF \left(\ln (\Gamma_R)/(\Gamma_O)\right)$$

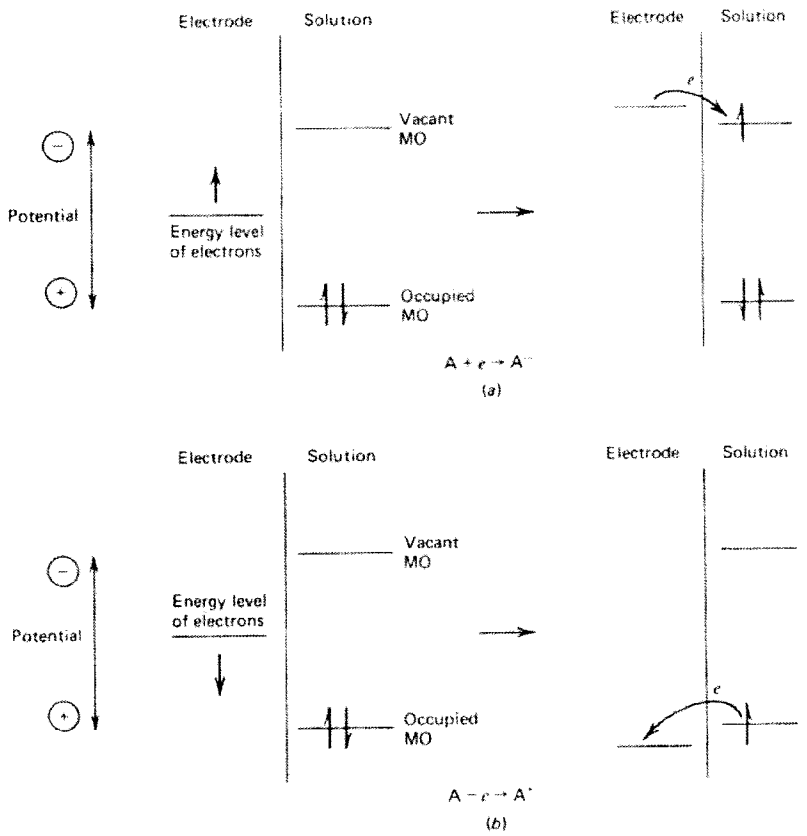

Figure 1.7: (a) Electron flow for a reduction and (b) Electron flow for an oxidation. Reprinted from reference 4.

In this equation, E is the electrode potential measured in volts, E° is the standard potential for the reaction also in volts, R is the ideal gas constant (8.3144 J/(mol-K), T is the temperature in Kelvin, n is the number of electrons transferred, F is Faraday's constant (96,485 C/mol), and Γ_R and Γ_O are the surface coverages of the reduced and oxidized species, respectively.[14]

An electrochemically reversible electron transfer reaction manifests in the difference in the anodic and cathodic peak potentials ($\Delta E_p = E_{p,a} - E_{p,c}$) being equal to 0 mV at all scan rates. In practice, ΔE_p is typically 5-10 mV for most electroactive SAMs and increases by a few mV with increasing scan rate due to uncompensated solution resistance.

If the electron transfer is kinetically slow, then the reaction is said to be electrochemically irreversible. The Butler-Volmer equation, which relates current to overpotential, can be used to extract the heterogeneous electron transfer rate constant when the overpotential is small. For self-assembled monolayers, the Butler-Volmer Equation takes the form:

$$i = nFAk^{\circ}[\Gamma_O \exp \alpha n f(E-E^{\circ'}) - \Gamma_R \exp (1-\alpha) n f(E- E^{\circ'})]$$

In this equation, i is the current measured in amperes, A is the area of the electrode measured in cm^2, k° is the standard heterogeneous electron transfer rate constant, α is the transfer coefficient (which is usually assigned to be 0.5), f is RT/F, $E-E^{\circ'}$ is the overpotential in volts, and $E^{\circ'} = |E_{pa} + E_{pc}| / 2$ in volts.[14]

An electrochemically irreversible electron transfer for a surface confined species will manifest as an increase in ΔE_p as a function of increasing scan rate.

k° can be calculated based on how ΔE_p increases with increasing scan rate according to the method of Laviron.[22, 23] The Laviron equation, which is a convenient expression of the Butler-Volmer equation, takes the following form:

$$1/m = (nF\nu)/(RT\, k^\circ)$$

Laviron calculated tables for 1/m (where m is the slope of the line in a plot of ΔE_p vs. scan rate) and $n\Delta E_p$ at different scan rates, allowing the value of k° to be obtained.[22, 23]

A chemically reversible electron transfer is defined as one in which only the forward and reverse reactions can be reversibly driven when a small overpotential away from $E^{\circ'}$ is applied. Thus, when all of the analyte reduced in the forward scan is re-oxidized in the reverse scan, the electron transfer is chemically reversible. Chemical reversibility is indicated when the experimentally measured ratio of the anodic to cathodic peak currents is 1. If this ratio deviates from 1, the reaction is chemically irreversible.

A chemically irreversible electron transfer occurs when not all of the species reduced in the forward scan are re-oxidized in the reverse scan, resulting in the ratio of anodic to cathodic peak currents deviating from 1 (see Figure 1.8). An example of a chemically irreversible electron transfer would be if the reduced form of the analyte is unstable and decomposes to an electroinactive molecule. A generic reaction for this would be as follows:

$$O + ne^- \rightarrow R \xrightarrow{k_{chem}} Z$$

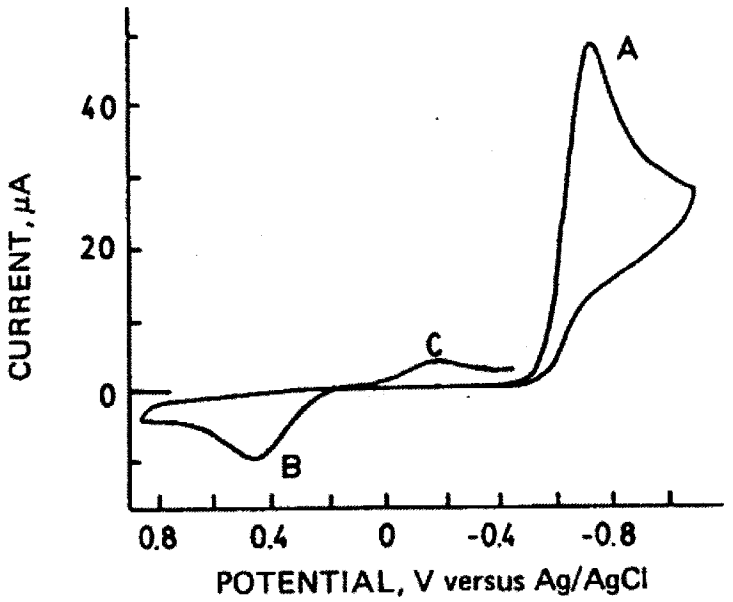

Figure 1.8: Voltammogram of chloramphenicol in an acetate buffer (.1 M). Reprinted from reference 28.

It is possible to determine the rate constant for a chemically irreversible process by increasing the scan rate or decreasing the temperature and observing the effect on the resulting voltammograms. Increasing the scan rate does not allow enough time for the chemical reaction to occur and lowering the temperature will slow down the reaction kinetics enough for the rate constant to be measured. At low scan rates or high temperatures, R has time to decompose to Z, resulting in no anodic current being observed. At intermediate scan rates or average temperatures, there is enough time for some of the R to decompose to Z, but not all of it. Thus, some of the R formed in the forward scan can be re-oxidized back to O. At high scan rates or low temperatures, there is no time for R to decompose to Z, so the anodic current will equal the cathodic current and the reaction will appear to be reversible. The rate constant for the chemical reaction can be obtained by proposing a mechanism for the decomposition of R to Z and simulating how changes in the scan rate or temperature changes the voltammetry. It is possible to find the rate constant by determining when the simulated voltammogram matches the experimental voltammogram. When that happens, the theoretical rate constant equals the actual rate constant. The proposed mechanism and value for k_{chem} must be verified by other methods because it is impossible to say if the simulated voltammogram is associated with only that reaction. It is possible that more than one reaction could give the same simulated voltammogram.

Cyclic voltammetry can also be used to measure a variety of thermodynamic properties associated with electron transfer. $E^{\circ'}$, the formal potential, which is related to the electronic structure of the analyte, can be determined by calculating an average of the anodic and cathodic peak potentials. $E^{\circ'}$ is an indicator of the electrochemical reactivity of the species because at that point half of the species are in the oxidized state and half of the species are in the reduced state.[14]

The surface coverages for the monolayer can be calculated by integrating the charge under a voltammetric wave, according to the equation[14]:

$$\Gamma = Q/(nFA\nu)$$

In this equation, Γ is the surface coverage in mol/cm^2, Q is the charge in coulombs , n is the number of electrons transferred, F is Farday's constant (96,500 C/equiv), A is the surface area is cm^2, and ν is the scan rate in V/s .[14] The surface coverage provides information on the number of electroactive sites on the surface, which is a measure of the packing density of the monolayer.

The width of the voltammetric wave at half-maximum (FWHM) is another important thermodynamic property because it directly correlates to the extent of ordering in the monolayer. If a monolayer is ordered and consists of non-interacting sites, then FWHM should theoretically be 90/n mV. If a monolayer is disordered, then the waves will broaden and FWHM values will increase. This arises because the electroactive sites in the SAM are in slightly different environments, yielding a distribution of $E^{\circ'}$'s and thus, broader peaks.

Ion-pairing constants can also be obtained by altering the concentration of the ion that forms ion-pairs in the presence of Y, an anion that is known not to form ion-pairs.[10] The excess electrolyte maintains the ionic strength in solution, which helps control changes in junction potential as the concentration of the active ion is changed. Some species form ion-pairs with the electrolyte when the species is oxidized or reduced.

$$A + X^- \rightarrow [A^+ \cdot X^-] + e^-$$

In this equation A is a neutral analyte molecule, X^- is a charge compensating anion, and $[A^+ \cdot X^-]$ is an ion pair between the oxidized form of A and an anion from the electrolyte. The ion-pairing constant, K_{eff}, is a measure of how strongly the ion-pair is bound together. By varying the concentration of the ion that forms the pair and seeing how the peak potential changes, K_{eff} can be calculated.[10] The relationship between the peak potential and the ion-pairing anion concentration is:

$$E_p = E_p' - (RT/nF) \ln (K_{eff} C_x)$$

In this equation, E_p' is the peak potential with no electrolyte X present, E_p is the peak potential with X present, and C_x is the initial concentration of the active ion.[10] Plots of E_p versus C_x should be linear, have a slope of 59/n mV, and have an intercept which is related to K_{eff}.[10]

Plots of current versus scan rate are important. If current is linear with respect to scan rate, then the species is surface confined. If current is linear with

respect to the square root of the scan rate, then the electron transfer is diffusion controlled, indicating that the electroactive species is in solution.

1.6 Ferrocenes and Ferrocene Containing Monolayers

An electroactive alkanethiol SAM contains an electroactive species attached as the terminal group. As with regular alkanethiol SAMs, the terminal group is connected to the headgroup by an alkyl chain of varying length, and the head group chemisorbs to the surface via a strong Au-S bond. These films are interesting because they can be studied using electrochemical methods such as CV and also because a variety of electroactive species can be attached as the terminal group. These monolayers can have many applications, such as sacrificial anodes, chemical and biological sensors and molecular electronic devices.[7] Ferrocene is a common choice for an electroactive group because it is easy to couple to alkanethiols and is a reversible, outer sphere redox couple which has been extensively characterized in the literature. Other electroactive terminal groups which have been studied include viologens, anthroquinones, porphyrins, oligoimides, and ruthenium pentammines.

Chidsey did pioneering work with mixed monolayers of $Cp_2FeCO_2(CH_2)_{11}SH$ and $CH_3(CH_2)_9SH$, as well as with "fully loaded" monolayers which contain only the electroactive thiol.[3] Fully loaded monolayers constructed from $Cp_2FeCO_2(CH_2)_{11}SH$ displayed broad voltammetric waves centered at approximately 580 mV. Replacement of the electron withdrawing ester group

with an electron donating methylene group caused the oxidation potential to shift cathodically by approximately 300 mV, as seen in the solution voltammetry of substituted ferrocenes.[3] In addition, the peaks observed for the methylene substituted ferrocene were observed to be much broader and asymmetric than those associated with the ester substituted alkanethiol. The surface coverages obtained by integrating the background corrected voltammetric peaks for a fully loaded ester substituted ferrocene monolayer were somewhat higher than that predicted by modeling the ferrocene group as a 6.6 Å sphere, possibly indicating that some of the ferrocene groups reside among the methylene chains.[3] Creager et. al. determined that the surface coverage of fully loaded films formed from $Cp_2Fe(CH_2)_6SH$ (which more closely resembles the monolayers reported here in) had a value of 4.6×10^{-10} mol/cm^{-2}, indicating a closely packed monolayer.[10]

The FWHM values observed by Chidsey and others, for undiluted monolayers, were much larger than the 90/n mV predicted for isolated, non-interacting sites.[3] This was attributed to the presence of defect sites in the monolayer. When defect sites are present, the ferrocene groups exist in many different environments, resulting in a broad distribution of $E^{\circ'}$'s and therefore FWHM values much larger than 90/n mV.[3]

The presence of defect sites in fully-loaded SAMs has also been inferred via the measurement of electron transfer kinetics. Several groups have demonstrated that electron transfer in such films is so rapid that the kinetics can not be measured on the voltammetric time scale, despite the presence of an

insulating alkane chain between the ferrocene and the electrode.[3, 4, 6] Ferrocene groups located at defect sites are closer to the gold surface, resulting in rapid electron exchange. Oxidation of the ferrocene moieties in more ordered regions of the SAM occurs via a fast electron-hopping mechanism to the more rapid sites (e.g. the electrons take the path of least resistance). Thus, electron transfer is electrochemically reversible.

A number of different types of defects are found in alkanethiol SAMs; step defects, tilt domain and grain boundary defects, and the poor packing shown by short alkyl chains are the most common types, as illustrated in Figure 1.9.[3] The presence of defects in the SAM can lead to problems with potential applications and therefore they are frequently eliminated entirely, or at least minimized, by preparing mixed monolayers.

One approach to minimizing the number of electroactive defect sites is co-adsorption with a large excess of electroinactive alkanethiols. In such a case, it is statistically less likely that a ferrocene group will occupy a defect site, resulting in more ideal voltammetry. The effectiveness of this approach was demonstrated by Chidsey et. al., when mixed monolayers of $Cp_2FeCO_2(CH_2)_{11}SH$ and decanethiol were prepared.[3] In these studies, the relative amounts of electroactive and electroinactive alkanethiols in the coating solution were varied and the resulting monolayers were examined via cyclic voltammetry. As the ratio of electroactive to electroinactive thiol was decreased, the surface coverage of the ferrocene substituted alkanethiol was found to decrease in proportion to it's

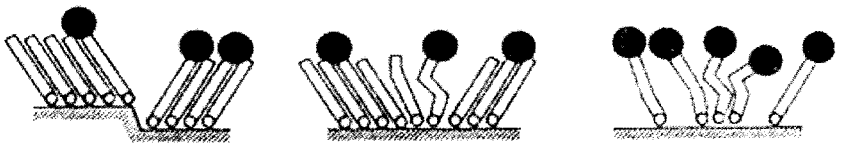

A B C

A. Crystal defects such as boundries or steps

B. Crystal domain boundry of an alkanethiol

C. Steric interactions

Figure 1.9: Electroactive sites in different environments. Reprinted from reference 4.

concentration in the coating solution.[3] The voltammetric peaks were also found to narrow, indicating an increase in order. When the mole fraction of the ferrocene containing alkanethiol in the coating solution was ≤0.25, the FWHM for the voltammetric waves reached the theoretical value of 90/n mV. In addition, a heterogeneous electron transfer rate constant of 5.2 s^{-1} was obtained when X_{Fe} = 0.1.[3] These results indicated that the electroactive sites in the monolayer were isolated and non-interacting, implying that all of the defect sites were occupied by decanethiol molecules.[3]

Another approach to obtaining defect free monolayers is to form the monolayers in the usual fashion, followed by soaking the resulting films in a solution containing only electroinactive alkanethiol. In this case, the electroactive thiols that occupy defect sites are replaced by electroinactive thiols, while those that are in crystalline domains stay in place (see Figure 1.10). Chidsey et. al. demonstrated that soaking monolayer coated electrodes in solutions of electroinactive alkanthiols resulted in an initial rapid exchange of active sites, followed by a slower decrease in coverage over a period of several days.[3] As the soaking time was increased, the voltammetric waves were observed to narrow and after a period of 10 days, Chidsey measured a heterogeneous electron transfer rate constant of 1.8 s^{-1} for $Cp_2FeCO_2(CH_2)_{16}SH$ containing mixed monolayers.[3]

Fox et. al. further demonstrated the ease with which molecules occupying defect sites can be replaced by soaking $Cp_2FeCO_2(CH_2)_{16}SH$ / $CH_3(CH_2)_{15}SH$

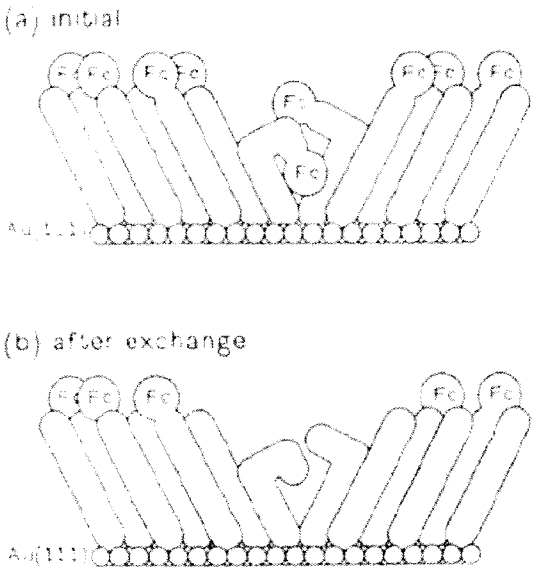

Figure 1.10: Tilt domain boundries (a) before and (b) after undergoing an exchange with a non-electroactive species. Reprinted from reference 3.

monolayers in solutions containing $Cp_2Fe(CH_2)_{16}SH$ and vice-versa.[24] In this case, the voltammetric peaks associated with the ester substituted ferrocene were found to decrease in proportion to the increasing signal for the alkyl substituted ferrocene (see Figure 1.11).[24] It was also observed that the peaks associated with oxidation/reduction of $Cp_2FeCO_2(CH_2)_{16}SH$ narrowed upon exchange, while those for $Cp_2Fe(CH_2)_{16}SH$ broadened (see Figure 1.11).[24]

Ion-pairing thermodynamics in mixed monolayers of $Cp_2Fe(CH_2)_6SH$ / $CH_3(CH_2)_nSH$ (5% $Cp_2Fe(CH_2)_nSH$, n = 4, 6, 8,10 and 12) were studied by Creager et. al.[10] It is well documented that ferrocinium forms tight ion-pairs with a variety of anions, including ClO_4^- and PF_6^-.[25, 26] The energetics associated with ion-pair formation in the unique environment presented by SAM's was explored by examining the anodic shift in peak potential in 1.0 M H_2SO_4 (aq) solutions containing decreasing amounts of perchloric acid.[10] 1.0 M H_2SO_4 (aq) was chosen as the background electrolyte to maintain the ionic strength of the solution, thus minimizing problems with changes in junction potentials. In addition, HSO_4^- (aq) (the predominate species in sulfuric acid solutions) does not form ion-pairs with ferrocinium.[10]

The reactions which describes ion-pair formation and the associated equilibrium constant (K_{eff}) are:

$$Cp_2Fe^+ + ClO_4^- \leftrightarrow Cp_2Fe^+ \cdot ClO_4^-$$

$$K_{eff} = [Cp_2Fe^+ \cdot ClO_4^-] / [Cp_2Fe^+][ClO_4^-]$$

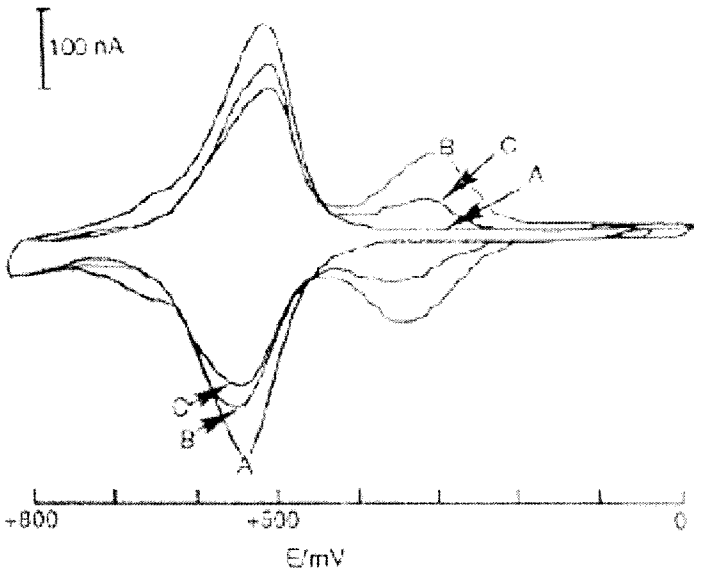

A. mixed thiol monolayer

B. after exchange with $HS(CH_2)_{16}Fc$

C. after then exchanging with $HS(CH_2)_{15}CH_3$

Figure 1.11: Cyclic voltammograms in 1 M aqueous perchloric acid, Ag/AgCl (saturate KCL) reference electrode, Pt wire counter electrode. Au/ $S(CH_2)_{16}OCOFc$ and $S(CH_2)_{15}CH_3$ mixed monolayer. Reprinted from reference 24.

K_{eff} was evaluated by measuring the peak potential as a function of perchloric acid concentration according to the equation[10]:

$$E_p = E_p^{'} - (RT/nF) \ln (K_{eff}C_x)$$

In this equation, E_p is the peak potential in 1.0 M H_2SO_4 (aq), $E_p^{'}$ is the peak potential when $HClO_4$ (aq) is present in the electrolyte, C_x is the concentration of $HClO_4$ (aq) and R,T, n, and F have their usual values.[10]

Plots of E_p vs. $\log_{10}$ [$HClO_4$] were constructed and analyzed via linear regression and the y-intercepts were used to calculate K_{eff}. The results demonstrated that as the length of the alkanethiol co-adsorbate increased, the ion-pairing constant increased dramatically from 870 M^{-1} for butanethiol and hexanethiol to 22,000 M^{-1} for dodecanethiol.[10] The increase in K_{eff} is a reflection of the increasingly "alkane-like" environment experienced by the Cp_2Fe groups as the chain length increases. The more non-polar environment stabilizes Cp_2Fe with respect to Cp_2Fe^+, making ion-pair formation more facile, thus increasing the value of K_{eff}.[10]

The slopes obtained from the plots of of E_p vs. $\log_{10}$ [$HClO_4$] were observed to deviate from the theoretical value of 59/n mV by approximately 5 mV/decade change in the concentration of $HClO_4$ (aq).[10] This was attributed to the fact that concentrations were used in data analysis, instead of activities.[10]

1.7 Oligoferrocenes and Oligoferrocene Containing Monolayers

Monolayers have also been made with compounds containing two ferrocene groups. As with other electroactive monolayers, the ferrocenes are attached as the terminal group of an alkanethiol. Usually the ferrocenes are not in equal electronic environments due to substituent effects, resulting in two distinct voltammetric peaks.

Filler made monolayers containing 1,2-diferrocenylethane separated from the electrode by chain lengths of 6, 12, and 16 carbons.[6] The cyclic voltammograms displayed two, one electron redox waves centered at 20 mV and 303 mV, with respect to a silver wire pseudo-reference electrode.[6] The wave centered at 20 mV was associated with oxidation of the outer ferrocene group, which had an electron donating methylene substituent, while the wave at 303 mV was determined to be for the inner ferrocene group due to an electron withdrawing carbonyl substituent. The reported values were different than those typically reported for carbonyl and methyelene substituted ferrocenes because a different reference electrode was employed.[6]

The surface coverages for all four waves were determined to be approximately 2.0×10^{-10} mol/cm^2, which is characteristic of a densely packed monolayer with a head group modeled as a 12 Å sphere.[6] The similar surface coverages for the inner and outer ferrocene groups indicated that all of the ferrocene groups were electrochemically accessible. In addition, the ratio of the

coverages for the anodic to cathodic peaks for each ferrocene was approximately 1, indicating that the electron transfer was chemically reversible.[6]

FWHM values for the redox waves were approximately 125mV for the inner ferrocene and approximately 155 mV for the outer ferrocene.[6] These values are greater than the 90/n mV predicted for isolated, non-interacting sites, but are smaller than those typically observed for fully loaded SAMs. This indicated that the films were disordered, but not as disordered as typical short chain electroactive monolayers.[6]

Examination of the variation in ΔE_p with respect to scan rate indicated that for all 3 of the monolayers studied (C6, C12, and C16), oxidation of the inner ferrocene group was reversible on the voltammetric time scale ($k^\circ > 20s^{-1}$). However, in each case oxidation of the outer ferrocene proved to be kinetically slow. The heterogeneous electron transfer rate constants for the C6, C12, and C16 derivatives were found to decrease with the logarithm of the number of methylene units, indicating that the monolayers possessed some order, even though they were not diluted with electroinactive diluent alkanethiols.[6]

Kubo also studied the redox behavior of bifferocene (Bfc) monolayers by attaching Bfc-$CO(CH_2)_7SH$ to Au (111) electrodes.[5] Two voltammetric peaks were observed, centered at 197 mV for the outer ferrocene and 666 mV for the inner ferrocene (see Figure 1.12).[5] Two peaks were observed due to the different substitution patterns on the ferrocene groups, as seen with other ferrocene containing films. The ferrocene surface coverage estimated from the

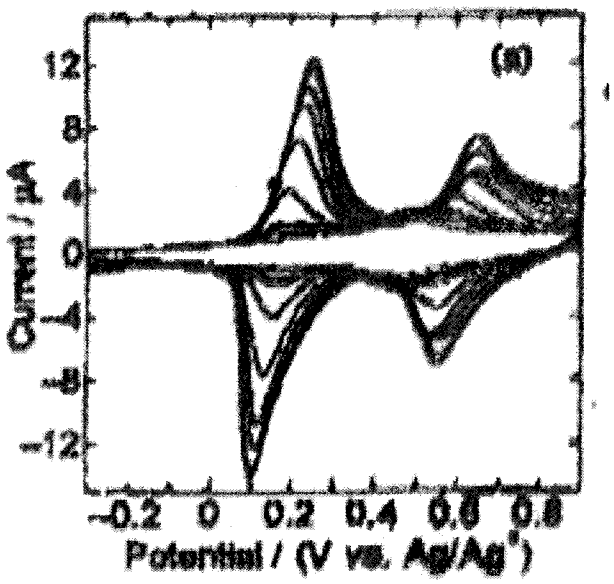

Figure 1.12: Cyclic Voltammogram of biferrocene Bfc^{+}/Bfc^{0} and Bfc^{2+}/Bfc^{+} couples in Bu_4NPF_6-CH_2Cl_2 on a Au (111) electrode. Consecutive scans at 0.1 V s^{-1}. Reprinted from reference 5.

Bfc^+/Bfc^0 couple was determined to be 4.6×10^{-10} mol cm^2, though the authors did not indicate why the coverage of the Bfc^{2+}/Bfc^+ couple was not reported. Based on a visual comparison, it appears that the surface coverages for the two peaks are approximately equal.[5]

The peak currents for both waves were found to decrease with increasing number of scans. Based on a plot of surface coverage vs. number of scans, it was determined that oxidation of Bfc^0 was chemically irreversible, obeying second order kinetics. Oxidation of Bfc^+ was also chemically irreversible, obeying first order kinetics.[5]

The electrochemical kinetics of the biferrocene monolayers were evaluated based on the method of Laviron.[22, 23] The heterogeneous electron transfer rate constants for the inner and outer ferrocenes were determined to be 0.64 s^{-1} and 0.93 s^{-1}, respectively.[5] This is an extremely unusual result because electron transfer from the inner ferrocene is actually slower, despite the fact that it is closer to the electrode. The authors speculated that this was the result of electrostatic interactions between the anion associated with the outer ferrocinium and the anion for the inner ferrocene.[5]

1.8 Research Proposal

The goal of this project involved the formation of monolayers of 6-(diferrocenylhexanylcarbonyl)pentanethiol on polycrystalline gold electrodes. Cyclic voltammetry was used to determine the thermodynamic and kinetic properties of the monolayer. Chemical and electrochemical kinetics were

evaluated by determining how the voltammetry changed as a function of scan rate. Thermodynamic properties, such as formal potentials, FWHM values, and surface coverages were also determined from the voltammograms.

Ion-pairing constants were measured as a probe of monolayer structure. Cyclic voltammograms in 1.0 M H_2SO_4 (aq) containing varying amounts of $HClO_4$ (aq) were obtained. The shift in formal potentials with decreasing [$HClO_4$] were measured and plots of $E^{\circ'}$ vs. $\log_{10}$ [$HClO_4$] allowed the magnitude of K_{eff} to be determined.

The effect of a non-aqueous electrolyte on the relative surface coverages for the inner and outer ferrocenes was evaluated by obtaining cyclic voltammograms in 0.10 M TBAP/THF electrolyte.

1.9 References

(1) Ulman, A. *Chem. Rev.* **1996**, *96*, 1533-1554.

(2) Poirier, G.; Pylant, D. *Science* **1996**, *272,* 1145-1148.

(3) Chidsey, C.E.D.; Bertozzi, C.R.; Putvinski, T.M., Mujsce, A.M. *J. Am. Chem. Soc.* **1990**, *112*, 4301-4306.

(4) Pugh, Carolyn A. Synthesis and Electrochemical Characterization of Novel Bridged Diferrocene Tagged Alkanethiol Self-Assembled Monolayers, M.S. Thesis, Youngstown State University, Youngstown, May 2001

(5) Kubo, K.; Hiroaki, K.; Hiroashi, N. *Electrochemistry* **1999**, *12*, 1129-1131.

(6) Filler, W. J. Characterization of Diferrocene Tagged Self-Assmebled Alkanethiol Monolayers M.S. Thesis, Temple University, August, 1996.

(7) Huc, V.; Bourgoin, J.; Bureau, C., Valin, F., Zalczer, G., Palacin, S. *J. Phys. Chem. B* **1999**, *103*, 10489-10495.

(8) Willicult, R.J.; McCarley, R.L. *J. Am. Chem. Soc.* **1994**, *116* (23), 10823-10824.

(9) Ulman, A. *An Introduction to Ultrathin Organic Films*; Academic Press: New York, **1994**.

(10) Rowe, G.K.; Creager, S. E. *Langmuir* **1991**, *7*, 2307-2312.

(11) Murray, R. W., *Electroanalytical Chemistry,* Vol. 13 A. J. Bard (Ed), Marcel Dekker, New York, **1984**, p. 91

(12) Nuzzo, R. G.; Fusco, F. A.; Allara, D. L. *J. Am. Chem. Soc.* **1987**, *109*, 2358-2368.

(13) Strong, L.; Whitesands, G.M. *Langmuir* **1988**, *4*, 546-558.

(14) Bard, A.; Faulkner, L. *Electrochemical Methods*; Wiley: New York, **1980**.

(15) Murray, R. *Molecular Design of Electrode Surfaces*; Wiley: New York, **1992**.

(16) Chidsey, C. E. D.; Gang-Yu, L.; Rowntree, P.; Giacinto, S. *J. Chem. Phys.* **1989**, *91*, 4421-4423.

(17) Tillman, N.; Ulman, A.; Schildkraut, J.S.; Penner, T. L. *J. Am. Chem. Soc.* **1988**, *111*, 6136.

(18) Rabe, J.P.; Knoll, W. K. *Opt. Commun.* **1986**, *57*, 189.

(19) Porter, M.D.; Bright, T. B.; Allara, D. L.; Chidsey, C. E. D. *J. Am. Chem. Soc.* **1987**, *109*, 3559.

(20) Brett, C. *Electrochemistry-Principles, Methods, and Applications*; Oxford University Press: New York, **1993**.

(21) Evans, D.J. *Chem. Educ.* **1983**, *60*, 290-293.

(22) Laviron, E. *J. Electroanal. Chem* **1979**, *101*, 19-28.

(23) Laviron, E. *J. Electroanal. Chem.* **1979**, *100*, 263-270.

(24) Collard, D.M., Fox, M. A. *Langmuir* **1991**, *7*, 1192-1197.

(25) Marcus, Y. *Ion Solvation*, Wiley and Sons: New York, **1985**; pp 107-109.

(26) Yang, E. S.; Chan, M. –S.; Wahl, A. C. *J Phys. Chem.* **1980**, *84*, 3094.

(27) Dean, J. C.; Herr, B. R.; Hulteen, J. C.; Van Duyne, R. P.; Mirken, C. A. *J. Am. Chem. Soc.* **1996**, *118*, 10211-10219.

(28) Kissinger, P.; Heineman, W. *J. Chem. Educ.* **1983**, *60*, 702-706.

CHAPTER 2:

FORMATION OF MONOLAYERS / ELECTROCHEMICAL INVESTIGATION

2.1 Introduction

This project involved making monolayers of 6-(diferrocenylhexanylcarbonyl)pentanethiol (DFHC6SH) on polycrystalline gold electrodes. A preliminary electrochemical investigation of these monolayers has been reported previously.[1] The goal of this project is to provide a more complete description of the electrochemical properties of self-assembled monolayers containing diferrocenylhexane terminal groups. A complete electrochemical study has allowed for exploration into possible practical applications such as in chemical and biological sensors.

The kinetic and thermodynamic quantities for monolayers of DFHC6SH were investigated via cyclic voltammetry. The voltammograms were analyzed for chemical and electrochemical reversibility and the results were compared to literature values. Thermodynamic properties such as formal potentials, surface coverages, FWHM values, and ion-pairing constants were also obtained and compared to the literature.

2.2 Experimental

2.2.1 Chemicals

DFHC6SH was prepared by Carolyn A. Pugh according to the method of Curtin et al.[1] 1 μm alumina oxide (Leco), perchloric acid (Fisher, Reagent A.C.S., 70%), sulfuric acid (Fisher, certified A.C.S. Plus, 95.9%), and tetra-*n*-butylammonium perchlorate (TBAP) (Fluka, 98%) were used as received. Methylene chloride (Fisher, certified A.C.S., 99.9%) and tetrahydrofuran (VWR, Reagent A.C.S., 99.5%) were distilled over calcium hydride and Na/benzophenone, respectively, and were used immediately. De-ionized water had R >18MΩ.

2.2.2 Instrumentation

A Bioanalytical Systems (BAS) 100W Potentiostat was used for cyclic voltammetry experiments in a single compartment cell. 1.6 mm diameter Au and Pt working electrodes, a Pt wire counter electrode, and aqueous Ag/AgCl and non-aqueous Ag/Ag^+ reference electrodes were purchased from Bioanayltical systems.

2.2.3 Monolayer Preparation

Gold electrodes were polished on a LeCloth flocked twill polishing cloth with an aqueous slurry of 1μm alumina oxide on a Leco VP-160 polisher/grinder for 2

hours at a time, at a rate of about 110-120 rpm. After polishing, the electrodes were sonicated for 10 minutes in DI water and subsequently rinsed with DI water. They were then left overnight in air.

The electrode surfaces were reduced electrochemically by cycling at least twenty-five times between –1500 mV and +1500 mV in 1.0 M $HClO_4$ (aq), ending at –1500 mV. The electrodes were subsequently rinsed with DI water and fresh 1.0 M perchloric acid. The cell was washed, rinsed, and filled with fresh perchloric acid. "Blank" scans were done in 1.0 M $HClO_4$ (aq) to ensure that the electrodes were suitably clean. These processes were repeated until no Faradaic voltammetry was observed in the blanks.

2.2.4 Monolayer Voltammetry

After a clean blank was obtained, the electrodes were cleaned again in 1.0 M $HClO_4$ (aq), as above, to ensure a fully reduced surface. The gold electrodes were then rinsed with DI water and methylene chloride and immersed overnight in a stirred 1 mM solution of 6-(diferrocenylhexanylcarbonyl)pentanethiol in methylene chloride. The resulting monolayer coated electrodes were then rinsed thoroughly with methylene chloride, de-ionized water, and electrolyte. The thermodynamics and chemical and electrochemical kinetics of the monolayers were evaluated by immersing the electrodes in fresh 1.0 M $HClO_4$ (aq) electrolyte, and then performing cyclic voltammetry over a potential range of

–150 mV to 800 mV at scan rates of 50, 75, 100, 150, 200, 300, 400, 500, 600, 700, 800, 900, and 1000 mV/s.

Ion pairing studies were performed by examining how the formal potential for ferrocene oxidation varied as a function of changing $HClO_4$ (aq) concentration in the presence of 1.0 M H_2SO_4 (aq) supporting electrolyte. Concentrations of 0.0997 M, 0.0658 M, 0.0327 M, 0.00997 M, 0.00648 M, 0.00326 M, 0.00120 M, 0.000741 M, 0.000335 M, and 0.000100 M perchloric acid in 1.0 M sulfuric acid were used. At each of these concentrations, scans were taken at 200 mV/s and 100 mV/s, over an appropriate potential range. All other conditions were kept constant. If the monolayer still exhibited stable voltammetry when the ion-pairing experiments were complete, then a scan rate study was done, as above, to evaluate chemical and electrochemical kinetics.

The effect of a non-aqueous solvent on the relative surface coverages displayed by the monolayer was evaluated in a THF solution containing 0.10 M tetra-*n*-butlyammonium perchlorate (TBAP). For these experiments, a non-aqueous silver/silver nitrate (THF) reference electrode and a platinum wire counter electrode were employed. The monolayers were formed and treated as above, and a scan rate study was performed in 1.0 M $HClO_4$ (aq). The cell and electrodes were then cleaned, rinsed with de-ionized water, acetone, THF, and electrolyte solution. The electrodes were then placed in fresh electrolyte and the monolayer voltammetry was evaluated over a suitable potential window at a scan

rate of 200 mV/s. Scans were repeated 20-30 times, or until the peaks broke down and were difficult to see, indicating that the monolayer had de-sorbed.

2.3 Results and Discussion

2.3.1 Cyclic Voltammetry of 6-(diferrocenylhexanylcarbonyl)pentanethiol Monolayers

Cyclic voltammetry of monolayers containing DFHC6SH yielded two sets of well-resolved peaks centered at approximately 90 mV and 390 mV (Figure 2.1). These peaks corresponded to the one-electron oxidation of the outer and inner ferrocene groups, respectively. The measured formal potentials agreed well with the literature values for solution and surface-confined substituted ferrocenes. The outer ferrocene was oxidized at less anodic potentials due to the electron donating alkyl substituent, even though it was farther from the electrode. The electron-withdrawing carbonyl substituent caused oxidation of the inner ferrocene moiety to occur at potentials positive of ferrocene, with approximately a 300 mV difference in $E^{\circ'}$ between methylene and carbonyl substituted ferrocenes, which is well documented in the literature.[2]

Monolayer voltammetry was often poorly defined and difficult to reproduce on a daily basis, as seen in Figure 2.2. The red/ox peaks for the outer ferrocene were typically less well defined than those for the inner ferrocene. Peaks were often broad and difficult to measure, and sometimes did not appear in the

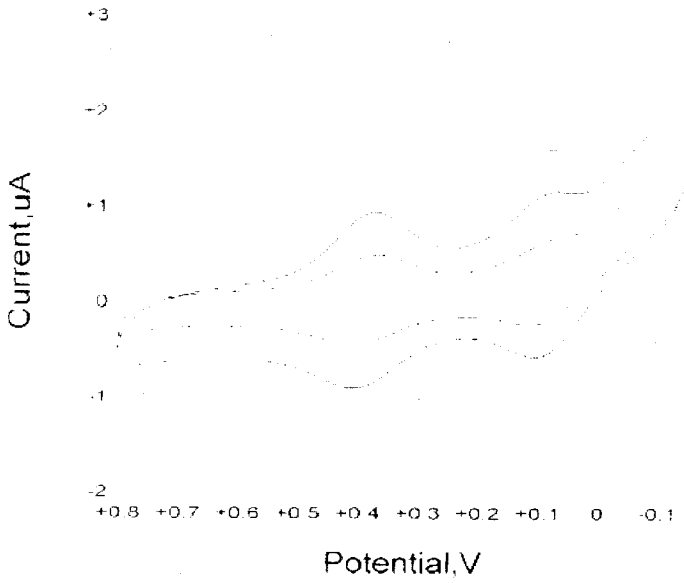

Line Color	Scan Rate
Blue	150 mV/s
Red	100 mV/s
Black	50 mV/s

Figure 2.1: Cyclic voltammogram of a good 6-(diferrocenylhexanylcarbonyl)pentanethiol self-assembled monolayer. Working electrode: Gold disc; Counter electrode: Platinum wire; Reference electrode: aqueous Ag/AgCl; Temperature 25°C.

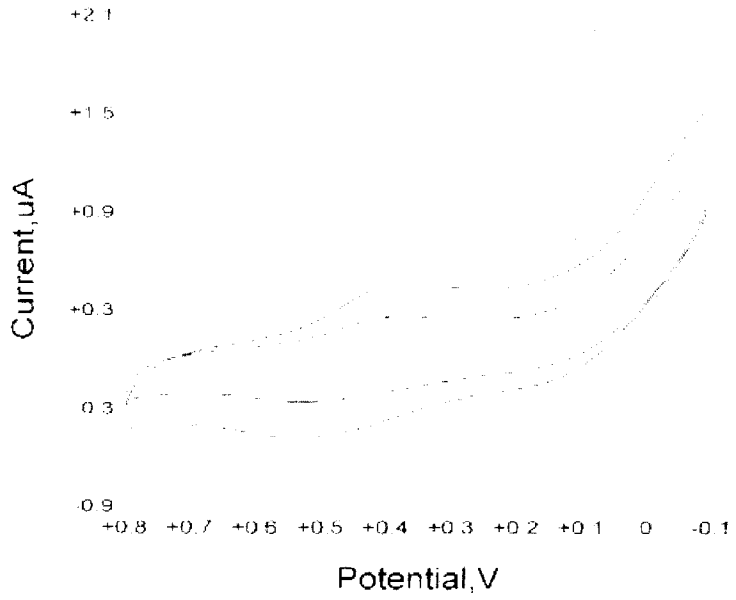

Line Color	Scan Rate
Blue	150 mV/s
Red	100 mV/s
Black	50 mV/s

Figure 2.2: Cyclic voltammogram of a poor 6-(diferrocenylhexanylcarbonyl)pentanethiol self-assembled monolayer. Working electrode: Gold disc; Counter electrode: Platinum Wire; Reference electrode: aqueous Ag/AgCl; Temperature 25°C.

voltammogram at all. Oxidation of the outer ferrocene occasionally yielded an extra peak at lower scan rates which merged with the wave associated with the inner ferrocene at higher scan rates. Problems with reproducibility were most likely due to the use of polycrystalline gold electrodes or disulfide formation in the coating solution over time.

The CV's were analyzed for surface-confinement by plotting i_p vs. υ for each wave. For scan rates from 50-1000 mV, the cathodic and anodic peaks showed a linear relationship between i_p and scan rate (Figures 2.3 and 2.4, respectively), indicating that electron transfer was from a surface confined species and was not diffusion controlled. The slopes of the i_p vs. υ plots are different for the inner and outer ferrocene groups due to the differences in their surface coverages, as indicated by the equation shown below.[3]

$$i_p = (n^2F^2A\Gamma/4RT)\upsilon$$

The surface coverages for the monolayer were obtained by integrating the background corrected current for each peak. Surface coverages indicated the number of electroactive sites on the electrode, which indicated the packing density at the monolayer. Typical numbers for the anodic and cathodic peaks associated with oxidation of the inner ferrocene (uncorrected for surface roughness) were -8.139×10^{-11} mol/cm^{-2} and 6.422×10^{-11} mol/cm^{-2}, respectively. Surface coverages for the anodic and cathodic peaks associated with oxidation of the outer ferrocene were -4.544×10^{-11} mol/cm^{-2} and 4.234×10^{-11} mol/cm^{-2}, respectively (see appendix A for a table of surface coverages). In previous

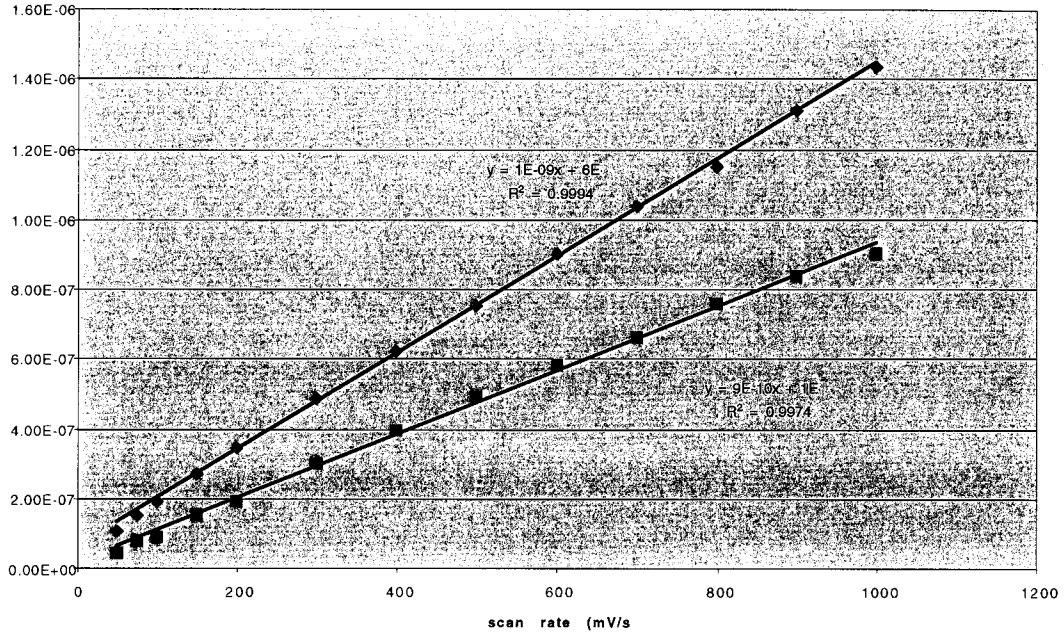

Figure 2.3: Plot of cathodic peak currents ($i_{p,c}$) versus scan rate (υ) for a good monolayer of 6-(differocenylhexanylcarbonyl)pentanethiol. _: inner ferrocene, _: outer ferrocene

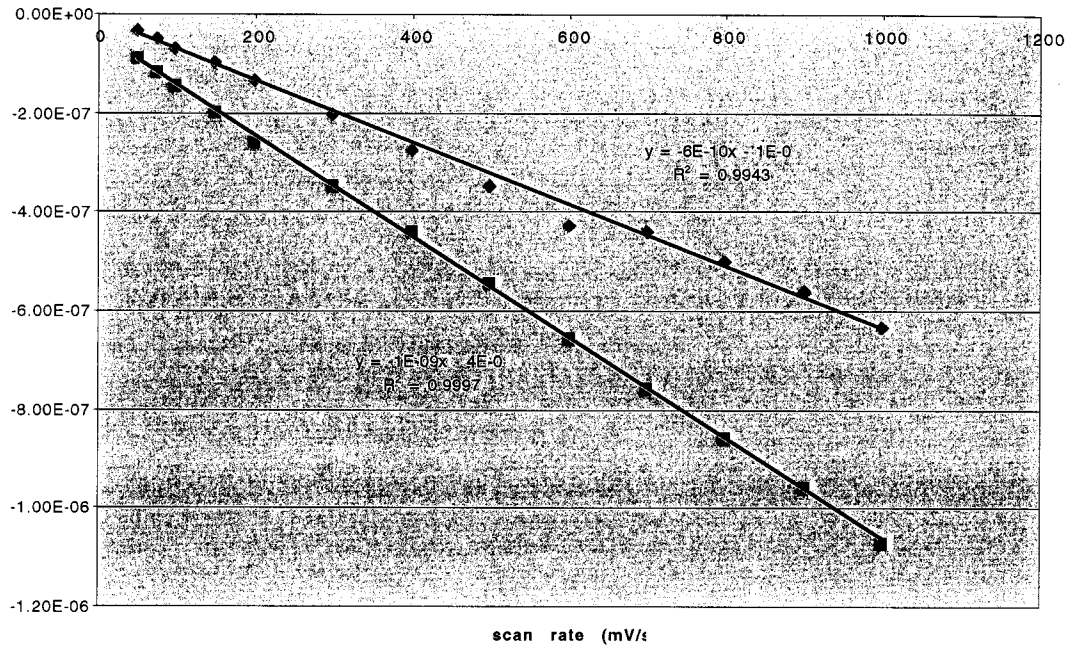

Figure 2.4: Plot of anodic peak currents ($i_{p,a}$) versus scan rate (υ) for a good monolayer of 6-(differocenylhexanylcarbonyl)pentanethiol. _: outer ferrocene, _: inner ferrocene

research with the same compound, Pugh[1] observed surface coverages that were slightly lower, probably because the voltammograms were extremely well defined. Surface coverages obtained for monolayers containing diferrocenylethane and biferrocene groups were approximately an order of magnitude higher than those observed for DFHC6SH monolayers.[4, 5] This is most likely due to the larger volume occupied by the diferrocenylethane or biferrocene head group.

The surface coverages for the inner and outer ferrocenes are not equal, which was unexpected. In general, surface coverages obtained for the outer ferrocenes were between 40-50% of those obtained for the inner ferrocene. This was also observed by Pugh in preliminary electrochemical experiments on DFHC6SH monolayers.[1] This was a very unusual result, because the coverages observed for the inner and outer groups in other dimeric ferrocene containing monolayers (diferrocenylethane and biferrocene), were approximately equal, indicating complete electrochemical accessibility for both red/ox active groups.[4, 5]

The observation that only 40-50% of the outer ferrocenes were electrochemically active was also unusual because it was opposite to the trend observed by Mirkin et. al. for monolayers containing an outer ferrocene directly bonded to an inner azobenzene group.[6] In this study, oxidation of the *outer* ferrocenes occurred readily, whereas reduction of the *inner* azobenzene groups was not observed at all. These results were rationalized by noting that the monolayers were very densely packed and it would therefore be extremely

difficult to force charge compensating cations into the film upon reduction of the azobenzene groups.[6]

Based on the work described above, it was expected that oxidation of the *inner* ferrocene group in DFHC6SH monolayers would be difficult, because forcing charge compensating anions into the bridging hexane group would be thermodynamically unfavorable. The opposite trend was observed in the voltammetry discussed above, indicating that the films were not densely packed and raising the question of why were all of the outer ferrocenes electrochemically not accessible? This could be due to the fact that the non-polar ferrocenes preferred the alkane environment presented by the bridging hexane group. Thus, the outer ferrocene groups might have folded into the non-polar hexane bridge, making them difficult to oxidize. Experiments designed to explore this theory were performed in non-aqueous electrolytes and are presented in Section 2.3.3. This theory could also be tested by the following experiments, which are beyond the scope of this work: STM to obtain images of the actual surface formed by the SAM, ellipsometry to measure the average thickness of the SAM, and surface infra-red measurements to probe the local environment around the ferrocenes. Another approach would be to synthesize compounds with a different structure such that the bridge is still non-polar, but rigid enough to prevent the folding of the outer ferrocenes into the non-polar region of the SAM.

The FWHM values for all peaks were greater than the theoretical prediction of 90/n mV for independent, isolated electroactive sites.[2] The FWHM values for the

anodic and cathodic peaks for the inner ferrocene were approximately 147 mV and 123 mV, respectively, while they were approximately 159 mV and 126 mV for the outer ferrocene. FWHM values of greater than 90/n mV indicate that disorder is present in the monolayer. In disordered films, ferrocene groups exist in a variety of different environments, resulting in a distribution of $E^{\circ'}$'s and therefore broad voltammetric waves. In previous studies of well-defined DFHC6SH monolayers, Pugh observed FWHM values of about 90 /n mV for oxidation of the inner ferrocenes, indicating a high degree of order in the film.[1] For the outer ferrocene groups, FWHM values for the anodic and cathodic peaks were 44.9 mV and 85 mV, respectively.[1] The sharpness of the anodic peak with respect to the cathodic peak for the outer ferrocenes could be indicative of a phase separation in the film upon oxidation of the outer ferrocene in well-ordered DFHC6SH SAMs.[7] The FWHM values obtained for films tagged with diferrocenylhexane are similar to those reported for monolayers containing diferrocenylethane and biferrocene head groups, indicating a similar degree of disorder in these films.[4, 5]

Chemical kinetics were also evaluated by determining the ratio of surface coverages (Γ_a/Γ_c) for both the inner and outer ferrocenes. As with most of the literature presented for ferrocene containing SAMs, this value was determined to be approximately 1 for the outer ferrocene, indicating that electron transfer was chemically reversible.[2,8,9] Γ_a/Γ_c for the inner ferrocene deviated from this value,

being approximately 0.8. However, this was attributed to the sloping background and peak tailing observed in the cathodic peak, and not to chemical irreversibility.

The electrochemical kinetics associated with oxidation of both ferrocenes were evaluated via the method of Laviron.[10, 11] In this method, the effect of increasing scan rate on ΔE_p was evaluated over a wide range of scan rates. If ΔE_p increased significantly with increasing scan rate, then a heterogeneous electron transfer rate constant could be determined.

In this study, ΔE_p for the inner ferrocene was approximately 40-80 mV. The observed deviation from the theoretical value of 0 mV was most likely due to uncompensated solution resistance. The value of ΔE_p was found to be completely independent of scan rate over a range of 50-1000 mV/s, indicating that the electron transfer was electrochemically reversible. The result is typical for ferrocene containing monolayers separated from the electrode by a chain containing six carbons, irrespective of the substituent attached to the ferrocene or the nature of the gold substrate.[1, 4, 8] From this data, it was possible only to say that the electron transfer rate constant was greater than 20 s^{-1}.

Evaluation of the electron transfer kinetics for oxidation of the outer ferrocene was somewhat ambiguous due to the fact that the peaks were broad and poorly defined, making an accurate determination of peak potentials difficult. ΔE_p for oxidation of the outer ferrocene group was also found to be between 40 and 80 mV, but was not always observed to be independent of scan rate over the range of 50 to 1000 mV/s. In about half of the experiments, ΔE_p was observed to

increase by approximately 15-25 mV with increasing scan rate, indicating a kinetically slow electron transfer. In the other half of the experiments, ΔE_p was found to be independent of scan rate, indicating a reversible electron transfer. Due to the frequent difficulty in accurately determining ΔE_p, and the fact that the increase in ΔE_p was small over a wide range of scan rates, it was chosen to conservatively report that oxidation of the outer ferrocene was electrochemically reversible. Previous research by Pugh[1] using DFHC6SH and Filler[4] using differocenylethane-C6SH yielded better defined peaks with unambiguous rate constants of 11.9 s^{-1} ($\pm$0.2) and 7.8 s^{-1} ($\pm$0.2 s^{-1}), respectively. These observations further imply that the monolayers reported in this study were somewhat disordered.

2.3.2 Ion-Pairing Thermodynamics

Ferrocene is known to form discrete ion-pairs with ions such as perchlorate and hexafluorophosphate.[8] The equilibrium constant for the ion-pairing reaction is derived from the following equation:

$$Cp_2Fe^+ + ClO_4^- \leftrightarrow Cp_2Fe^+ \cdot ClO_4^-$$

$$K_{eff} = [Cp_2Fe^+ \cdot ClO_4^-] / [Cp_2Fe^+][ClO_4^-]$$

The magnitude of the equilibrium constant is a measure of the polarity of the medium in which the red/ox reaction occurs.[8] If the medium is more non-polar, then the ferrocene becomes more stable with respect to ferrocinium, which results in a positive shift in $E^{\circ\prime}$. The value for K_{eff} indicates the thermodynamic

cost for forcing a positively or negatively charged ion to be in an environment which is thermodynamically unfavorable (eg. an alkane).[8]

Monolayers of DFHC6SH were studied for their ion-pairing properties with a modified version of the method of Creager et. al.[8] The formal potential for both ferrocene groups were measured at scan rates of 100 mV/s and 200 mV/s with decreasing concentrations of $HClO_4$ (aq) in 1.0 M H_2SO_4 (aq). H_2SO_4 (aq) was chosen as the background electrolyte because it has been well-documented that HSO_4^- does not form an ion pair with ferrocinium.[8] For the Creager project, ΔE_p was approximately 0 mV, however, in this research ΔE_p typically varied between 40-80 mV.[8] As a result, $E^{\circ'}$ was measured rather than E_p because it was a better indicator of when half the sites existed as ferrocene and half existed as ferrocinium.

Cyclic voltammograms of the same DFHC6SH monolayer in 1.0 M $HClO_4$(aq) and in 1.0 M H_2SO_4 (aq) are shown in Figure 2.5. The formal potentials for both ferrocenes in 1.0 M H_2SO_4 (aq) were shifted anodically by approximately 125 mV with respect to $HClO_4$(aq), as also seen by Creager et. al.[8] Positive shifts in $E^{\circ'}$ were observed for all four voltammetric waves, indicating that the shift was thermodynamic in nature.

Voltammograms of DFHC6SH in 1.0 M H_2SO_4 (aq) with varying concentrations of $HClO_4$ (aq) are shown in Figure 2.6. An anodic shift in $E^{\circ'}$ was observed for both ferrocene groups with decreasing concentrations of $HClO_4$ (aq), as observed by Creager et. al.[8] In general, the voltammetric waves were

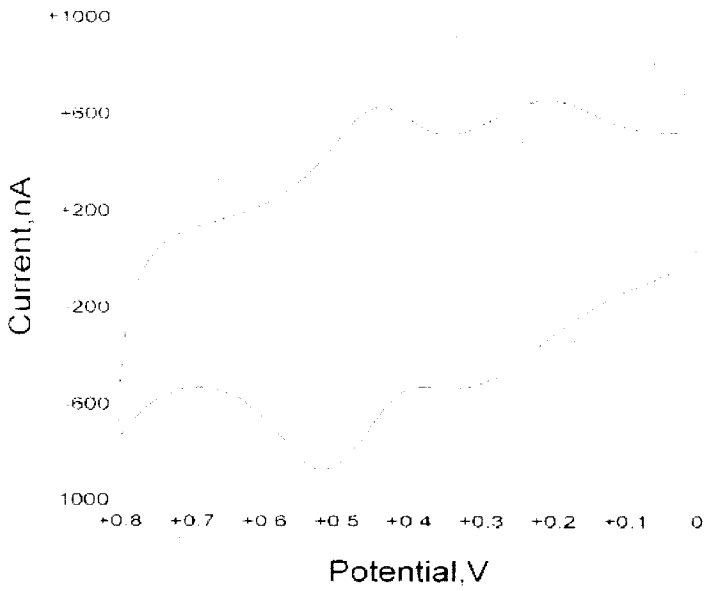

Line Color	Acid
Blue	1.0 M perchloric acid
Red	1.0 M sulfuric Acid

Figure 2.5: Cyclic voltammograms of a 1.0 mM of 6-(diferrocenylhexanylcarbonyl)pentanethiol self-assembled monolayer. Working electrode: Gold disc; Counter electrode: Platinum Wire; Reference electrode: aqueous Ag/AgCl; Temperature 25°C.

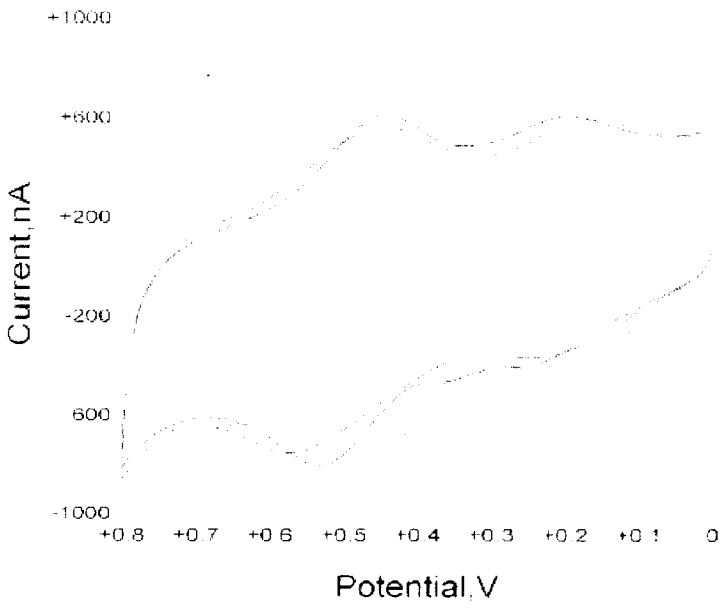

Line Color	Concentration
Blue	.0997 M perchloric acid
Red	.00997 M perchloric acid
Black	.00120 M perchloric acid

Figure 2.6: Cyclic voltammogram of 6-(diferrocenylhexanylcarbonyl)pentanethiol self-assembled monolayer. Working electrode: Gold disc; Counter electrode: Platinum Wire; Reference electrode: aqueous Ag/AgCl; Temperature 25°C.

better defined in the 1.0 M $HClO_4$(aq) than the 1.0 M H_2SO_4 (aq). As the concentration of $HClO_4$ (aq) was decreased, the peaks were observed to broaden and become poorly defined, especially for the outer ferrocene. In addition, the voltammetric waves frequently disappeared or formed multiple peaks at lower $HClO_4$(aq) concentrations. The voltammetric waves for the 4 lowest concentrations of $HClO_4$ (aq) were often so poorly defined that it was impossible to obtain accurate measurements for E°', so these values were not included in the determination of K_{eff} (see appendix B for tables of K_{eff}'s).

The following equation was used to calculate K_{eff} from E°':

$$E°' = E°'* - (RT/nF) \ln (K_{eff} [ClO_4^-])$$

Where E°'* is the formal potential in 1.0 M H_2SO_4 (aq) and E°' is the formal potential measured for each monolayer in 1.0 M H_2SO_4 (aq) with varying concentrations of $HClO_4$ (aq).[8] Typical plots of E°' vs. $\log_{10} [ClO_4^-]$ for both the inner and outer ferrocene can be seen in Figures 2.7 and 2.8. The intercepts and slopes obtained from these plots via linear regression analyses were used to calculate K_{eff}. The K_{eff}'s for the inner and outer ferrocenes were determined to be 13.06 M^{-1} and 3.915 M^{-1}, respectively. These results are averages obtained from four separate monolayers and the standard deviations for the inner and outer ferrocenes were 11.52 and 2.773, respectively. The large standard deviations observed for both values of K_{eff} were a reflection of the difficulties in obtaining well-defined, reproducible voltammetry, as discussed in section 2.3.1. Because of the difficulty in measuring the peak potentials accurately, the values given for

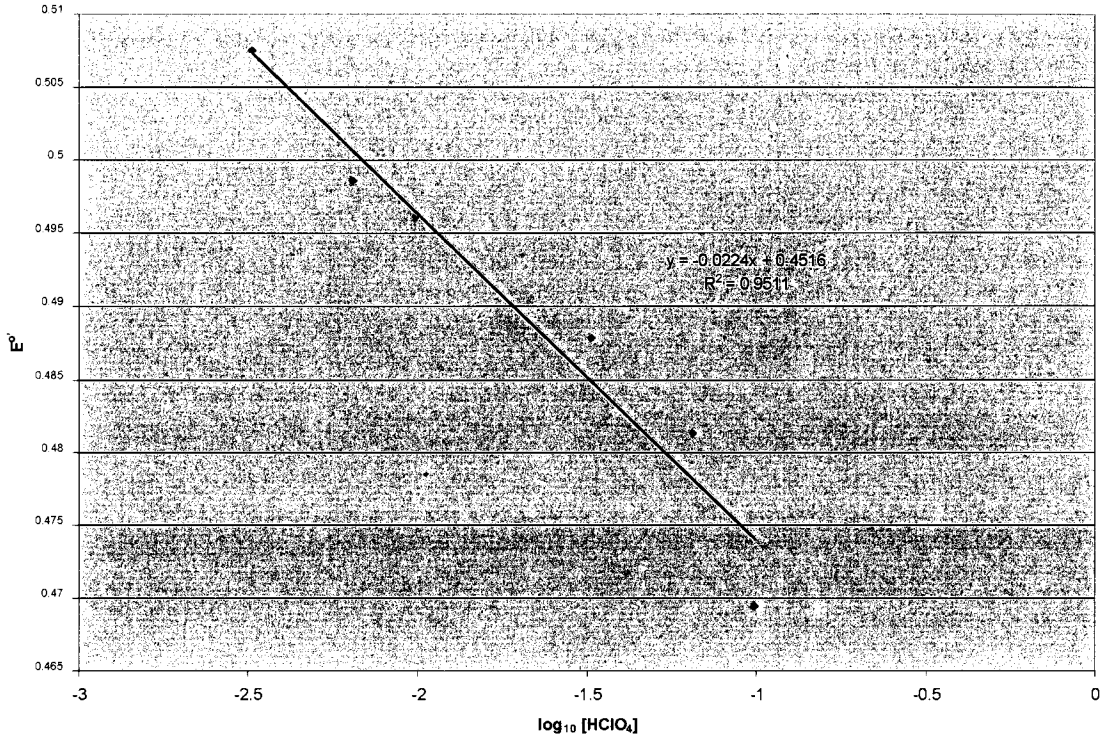

Figure 2.7: Plot of E_i° vs. $\log_{10}[HClO_4]$ for the inner Cp_2Fe.

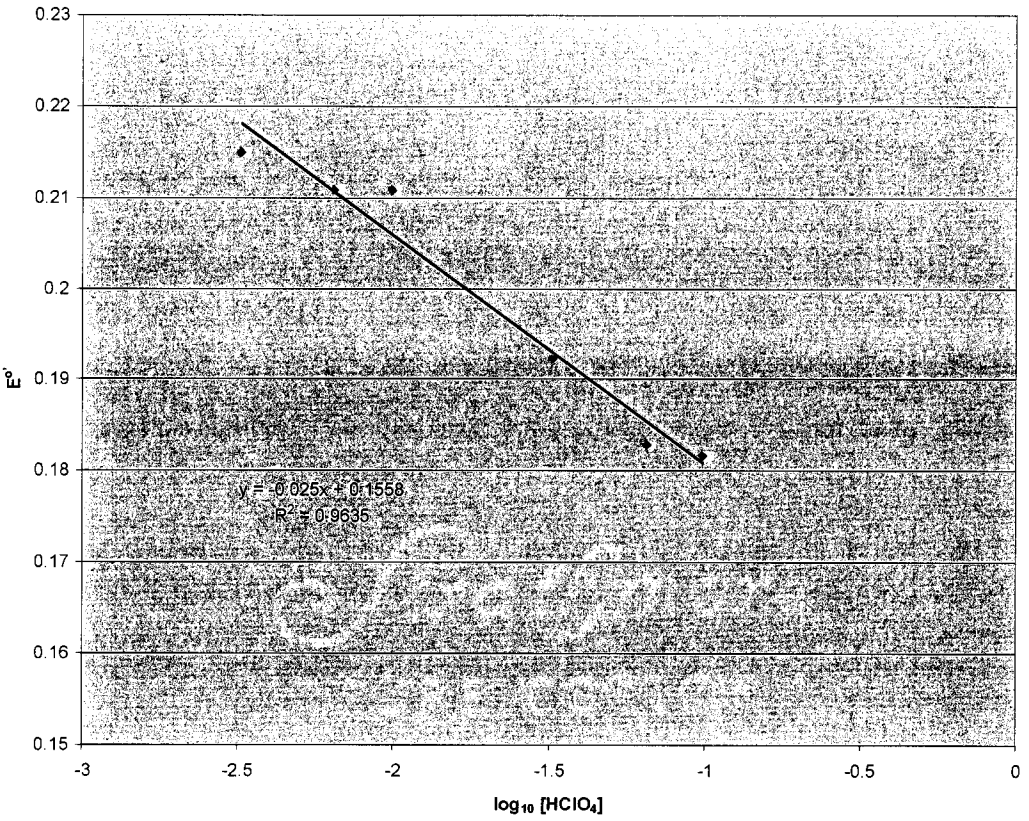

Figure 2.8: Plot of E_i° vs. $\log_{10}[HClO_4]$ for the outer Cp_2Fe.

K_{eff} should not be considered quantitative, the important thing to notice are the trends that are observed.

The slopes for graphs of $E^{\circ'}$ vs. $\log_{10}[ClO_4^-]$ were significantly less than the expected value of 59/n mV, and the graphs were not linear.[8] Creager[8] also saw graphs that were not linear. As a result of these inconsistencies, the values obtained for K_{eff} should not be treated as quantitative. The observed trends in K_{eff}, however, are valid. Further experiments will be done to explain this phenomenon.

The observation that K_{eff} for the inner ferrocene is larger than that for the outer ferrocene is not overly surprising given that the inner ferrocene groups are shielded from the aqueous electrolyte by the bridging hexane group. The magnitude of the ion-pairing constant for the inner ferrocene is significantly lower than the value of 22, 000 M^{-1} reported by Creager[8] for dilute mixed monolayers of ferrocenehexanethiol and dodecanethiol. This large difference in K_{eff} is representative of the dramatic differences in monolayer structure in the two studies. In both instances, the electroactive group is buried in alkyl groups which are six methylene units in length. However, it is well documented that dilute mixed monolayers form structures that are much more highly ordered than those obtained for "fully loaded" films.[2] Thus, the local environment observed by the ferrocenes in Creager's work is expected to be *much* more non-polar than that in the current study, manifesting in a much larger value of K_{eff}.[8] The small values of K_{eff} for both ferrocene groups in fully loaded DFHC6SH monolayers, was thus

reflective of the increase in disorder found in these films. This disorder yielded monolayers much more porous to the electrolyte, resulting in a less "alkane-like" environment and a lower value of K_{eff}.

2.3.3 Monolayer Electrochemistry in Non-Aqueous Solvents

The effects of non-aqueous electrolytes on the electrochemical accessibility of the inner and outer ferrocenes were evaluated by comparing the relative surface coverages in aqueous $HClO_4$ and THF solutions containing 0.10 M TBAP. Recall that in 1.0 M $HClO_4$ (aq), only approximately 40-50% of the outer ferrocene groups were available for oxidation and that this behavior was not observed in diferrocenylethane tagged alkanethiol SAMs.[4] It was hypothesized that this could be due to the non-polar ferrocenes preferring the alkane-like environment presented by the hexane bridge, and may therefore fold over into the non-polar region, resulting in electrochemical inaccessibility. To test this theory, cyclic voltammetry of DFHC6SH monolayers in 0.10 M TBAP/THF solution was obtained. By placing the monolayer in a relatively non-polar environment, the outer ferrocene groups should unfold out of the hexane bridge and become electrochemically accessible. Thus, the ratio of the surface coverages for the inner and outer ferrocenes should increase and approach a value of one.

Monolayer voltammetry has been studied in non-aqueous media, but to a lesser degree than in aqueous media because the response is not stable over

time. In general, alkanethiol monolayers desorb in experiments performed in non-aqueous media after just a few voltammetric scans, resulting in a complete loss of faradaic response.

DFHC6SH monolayers were prepared and fully characterized in 1.0 M $HClO_4$ (aq), as previously described. They were then analyzed in 0.10 M TBAP/THF electrolyte at a scan rate of 200 mV/s. A typical first scan is shown in Figure 2.9 and a comparison between the voltammetry in aqueous and non-aqueous electrolytes is shown in Figure 2.10. The formal potentials of the inner and outer ferrocene were shifted cathodically by approximately 435 mV and 340 mV in non-aqueous media, respectively. This was most likely due to the different reference electrode which was employed, but might also have reflected the better solvation of ferrocene in THF.

Figure 2.11 shows the initial scan in 0.10 M TBAP/THF, as well as the 3^{rd} and 7^{th} scan. The figure demonstrates that the voltammetric response decreased with increasing number of scans due to desorption of the monolayer. The Faradaic response of the monolayer was typically observed to completely disappear after 20-30 scans in the non-aqueous electrolyte solution.

The most important observation about Figure 2.10 was that, within experimental error, the relative surface coverages for oxidation/reduction of the inner and outer ferrocenes remained the same in non-aqueous electrolytes, even though the actual coverages decreased by approximately 40-60% due to

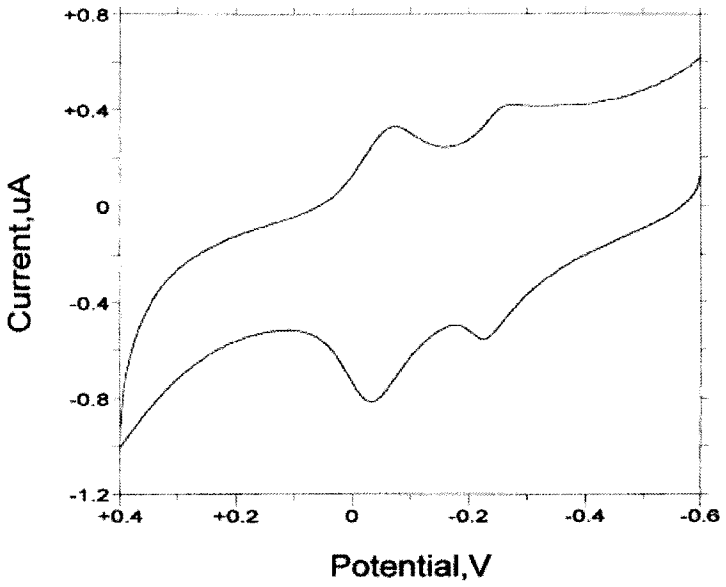

Figure 2.9: Cyclic voltammogram of the first scan of a 6-(diferrocenylhexanylcarbonyl)pentanethiol self-assembled monolayer in .10 M TBAP/THF solution. Working electrode: Gold disc; Counter electrode: Platinum Wire; Reference electrode: non-aqueous Ag/$AgNO_3$; Temperature 25°C.

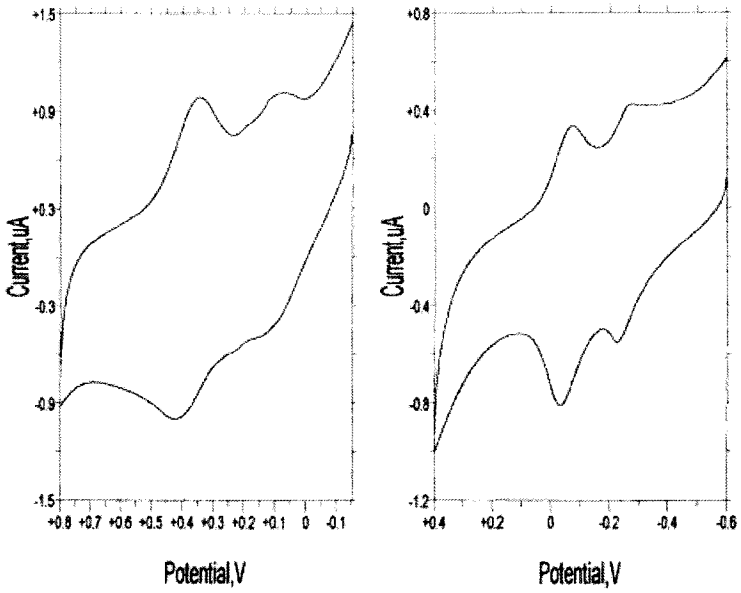

L voltammogram in 1.0 M perchloric acid
R voltammogram in .10 M TBAP in THF

Figure 2.10: Comparison of the cyclic voltammograms of 6-(diferrocenylhexanylcarbonyl)pentanethiol self-assembled monolayer in .10 M TBAP/THF solution and 1.0 M $HClO_4$ (aq). Working electrode: Gold disc; Counter electrode: Platinum Wire; Reference electrode: aqueous Ag/AgCl (left), non-aqueous $Ag/AgNO_{3\ (right)}$; Temperature 25°C.

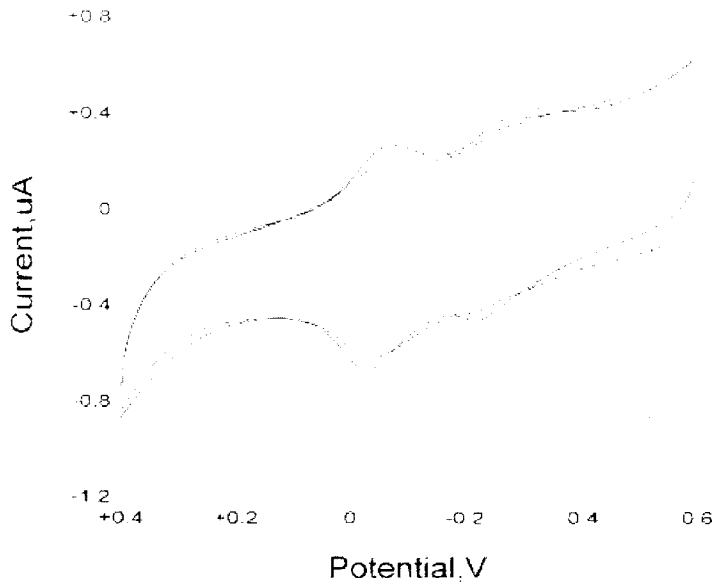

Line Color	Scan Number
Blue	1
Red	3
Black	7

Figure 2.11: Cyclic voltammogram of a 6-(diferrocenylhexanylcarbonyl)pentanethiol self-assembled monolayer in .10 M TBAP/THF solution. Working electrode: Gold disc; Counter electrode: Platinum Wire; Reference electrode: non-aqueous $Ag/AgNO_3$; Temperature 25°C.

desorption (see Appendix C and D). This result implied, but did not prove, that the reason why some of the outer ferrocenes were not electrochemically accessible was not due to folding into the hexane bridge. Further experiments in less polar solvents, along with those outlined in section 2.3.1 will be required to fully explain this very unusual phenomenon in self-assembled alkanethiol monolayer chemistry.

2.4 Conclusions

Cyclic voltammetry of SAMs containing DFHC6SH revealed that the outer ferrocenes were oxidized at less anodic potentials than the inner ferrocenes, despite the fact that they were farther from the electrode. It was determined that this was due to substituent effects; the electron donating alkyl substituent made the outer ferrocenes easier to oxidize. The measured formal potentials of approximately 90 mV and 390 mV (vs Ag/AgCl) were typical of substituted ferrocenes.

FWHM values for all of the voltammetric waves were found to be larger than the theoretical value of 90/n mV predicted for non-interacting electroactive sites. This indicated that the monolayers were somewhat disordered, a conclusion that was further supported by the fast electron transfer kinetics and ion-pairing studies, as discussed below.

The ferrocene oxidations were found to be chemically reversible, as expected for ferrocene containing monolayers. Electron transfer from the inner ferrocene

was determined to be electrochemically reversible on the voltammetric time scale. The electron transfer kinetics for the outer ferrocene, however, were not as clear cut. ΔE_p sometimes displayed a small (c. a. 15-25 mV) increase with increasing scan rate. The poor definition of the peaks associated with oxidation of the inner ferrocenes made an accurate determination of the peak potentials difficult. Thus, it was conservatively reported that the electron transfer for the outer ferrocene was also electrochemically reversible.

The most interesting aspect of the monolayer voltammetry was that the surface coverages for the inner and outer ferrocene moieties were not equal. The values indicated that only 40-50% of the outer red/ox sites were electrochemically accessible, a result which was opposite to that reported by Mirken et. al.[6] for monolayers containing ferrocene and azobenzene groups. This was possibly due to the non-polar ferrocenes preferring the "alkane-like" environment presented by the hexane bridge over the aqueous based electrolyte. Thus, the ferrocenes may have folded over into the bridge and their release was perhaps kinetically slow.

This theory was tested by performing the voltammetry in non-aqueous electrolytes. The results demonstrated that while surface coverages for both ferrocenes decreased due to desorption in the THF, the *ratio* of the coverages for the inner and outer groups remained constant. This limited set of data indicated that the electrochemical inaccessibility of the outer ferrocenes was probably not due to folding into the hexane bridge. Further experiments in less polar solvents

will be needed to clarify this issue. In addition, STM, surface infra-red, and ellipsometry studies may also be required.

Ion-pairing thermodynamics were also measured as a further probe of monolayer structure. The magnitude of the equilibrium constants determined in this study were much smaller than those reported by Creager et. al.[8] for mixed monolayers of ferrocenehexanethiol and various non-electroactive thiols. This indicated that fully-loaded DFHC6SH monolayers were much more porous to the electrolyte and were therefore disordered.

2.5 Future Work

A future goal of this project is to obtain more clearly defined voltammetry for DFHC6SH monolayers. This will be accomplished by adsorption onto Au(111) single crystal electrodes, rather than polycrystalline gold electrodes. In addition, disulfide which has formed in the coating solution will be converted back to the thiol before adsorption. These changes should give rise to more ordered monolayers and therefore improved definition for the voltammetric waves. Once high quality monolayers have been obtained, all of the experiments outlined above will be repeated.

In addition, the electrochemical inaccessibility of the outer ferrocene groups will be explored by examining the voltammetry in solvents which are less polar than THF. Ellipsometry, surface infra-red spectroscopy, and scanning tunneling

microscopy may be performed in collaboration with Dr. Robin L. McCarley at Lousiana State University.

2.6 References

(1) Pugh, Carolyn A. Synthesis and Electrochemical Characterization of Novel Bridged Diferrocene Tagged Alkanethiol Self-Assembled Monolayers, M.S. Thesis, Youngstown State University, Youngstown, May 2001.

(2) Chidsey, C.E.D.; Bertozzi, C.R.; Putvinski, T.M., Mujsce, A.M. *J. Am. Chem. Soc.* **1990**, *112*, 4301-4306.

(3) Bard, A.; Faulkner, L. *Electrochemical Methods*; Wiley: New York, **1980**.

(4) Filler, W. J. Characterization of Diferrocene Tagged Self-Assmebled Alkanethiol Monolayers, M.S. Thesis, Temple University, August, 1996.

(5) Kubo, K.; Hiroaki, K.; Hiroashi, N. *Electrochemistry* **1999**, *12*, 1129-1131.

(6) Dean, J. C.; Herr, B. R.; Hulteen, J. C.; Van Duyne, R. P.; Mirken, C. A. *J. Am. Chem. Soc.* **1996**, *118*, 10211-10219.

(7) P. J. Peerce; Bard, A. J. *J. Electroanal. Chem.* **1980**, *114*, 89.

(8) Rowe, G.K.; Creager, S. E. *Langmuir* **1991**, *7*, 2307-2312.

9) Finklea, H. O.; Hanshew, D. D. *J. Am. Chem. Soc.* **1992**, *114*, 3173-3181.

(10) Laviron, E. *J. Electroanal. Chem* **1979**, *101*, 19-28.

(11) Laviron, E. *J. Electroanal. Chem.* **1979**, *100*, 263-270.

Appendix A

Surface coverages	mol/cm^2	mol/cm^2
Day	peak 2	peak 3
2-Nov-01, E4	-7.874E-11	8.575E-11
08-Jun-01, E4	-1.155E-10	8.461E-11
08-Sept-01, E3	-5.381E-11	5.791E-11
08-Aug-01, E4	-5.856E-11	5.147E-11
28-Aug-01, E4	-1.185E-10	6.008E-11
22-Oct-01, E3	-6.856E-11	8.709E-11
08-Aug-01, E3	-5.394E-11	5.101E-11
22-Jun-01, E4	-1.035E-10	3.580E-11
Average	-8.139E-11	6.422E-11

Appendix B

Inner Ferrocene

Day	K_{eff} (M^{-1}) omitting last 3 pts.	K_{eff} (M^{-1}) omitting last 4 pts.
E3 10-Nov-01	4.012	4.204
E3 20-Nov-01	23.07	26.12
E4 20-Nov-01	15.67	19.32
E4 8-Jan-02	1.443	2.582
Average	11.05	13.06
Standard Deviation (s)	10.13	11.52
Relative Standard Deviation (RSD)	916.7	882.1

Outer Ferrocene

Day	K_{eff} (M^{-1}) omitting last 3 pts.	K_{eff} (M^{-1}) omitting last 4 pts.
E3 10-Nov-01	4.764	5.461
E3 20-Nov-01	2.027	1.530
E4 20-Nov-01	3.950	7.039
E4 8-Jan-02	.8723	1.629
Average	2.903	3.915
Standard Deviation (s)	1.775	2.773
Relative Standard Deviation (RSD)	611.4	708.3

Appendix C

Date	Solvent	Peak 1 Surface coverage (mol/cm^2)	Peak 2 Surface coverage (mol/cm^2)	Peak 3 Surface coverage (mol/cm^2)	Peak 4 Surface coverage (mol/cm^2)
8-Sept-01	1.0 M $HClO_4$ (aq)	-2.647e-11	-5.451e-11	6.041e-11	3.064e-11
	.10 M TBAP in THF	-2.197e-11	-5.273e-11	3.018e-11	1.910e-11
22-Aug.-01	1.0 M $HClO_4$ (aq)	-8.049e-11	-1.054e-10	4.791e-11	1.455e-11
	.10 M TBAP in THF	-2.482e-11	-3.320e-11	2.062e-11	1.214e-11
14-Aug.-01	1.0 M $HClO_4$ (aq)	-3.946e-11	-9.384e-11	8.227e-11	9.972e-12
	.10 M TBAP in THF	-1.885e-11	-4.820e-11	1.941e-11	1.792e-11
16-Aug.-01	1.0 M $HClO_4$ (aq)	-3.624e-11	-7.902e-11	7.459e-11	2.187e-11
	.10 M TBAP in THF	-2.092e-11	-4.938e-11	2.763e-11	8.116e-12
10-Aug.-01	1.0 M $HClO_4$ (aq)	-1.473e-10	-1.481e-10	1.773e-10	8.003e-11
	.10 M TBAP in THF	-8.822e-11	-8.624e-11	8.384e-11	5.616e-11

Appendix D

Date	Surface Coverage ratio	1.0 M $HClO_4$ (aq)	TBAP 1	TBAP 2	TBAP 3
8-Sept-01	Peaks ½	.49	.41	.52	.55
	Peak 4/3	.51	.63	.69	.83
22-Aug.-01	Peaks ½	.76	.75	.71	.65
	Peaks 4/3	.30	.59	.51	.64
14-Aug.-01	Peaks ½	.42	.39	.30	.25
	Peaks 4/3	.83	.92	.95	.77
16-Aug.-01	Peaks ½	.46	.42	.41	.44
	Peaks 4/3	.29	.29	.34	.32
10-Aug.-01	Peaks ½	.99	1.02	.95	1.45
	Peaks 4/3	.45	.67	.44	.35